

Post-Newtonian expansion of the spin-precession invariant for eccentric-orbit non-spinning extreme-mass-ratio inspirals to 9PN and e^{16}

Christopher Munna^{1,2} and Charles R. Evans²

¹*MIT Kavli Institute, Massachusetts Institute of Technology, Cambridge, MA 02139, USA*

²*Department of Physics and Astronomy, University of North Carolina, Chapel Hill, North Carolina 27599, USA*

We calculate the eccentricity dependence of the high-order post-Newtonian (PN) expansion of the spin-precession invariant ψ for eccentric-orbit extreme-mass-ratio inspirals with a Schwarzschild primary. The series is calculated in first-order black hole perturbation theory through direct analytic expansion of solutions in the Regge-Wheeler-Zerilli formalism, using a code written in MATHEMATICA. Modes with small values of l are found via the Mano-Suzuki-Takasugi (MST) analytic function expansion formalism for solutions to the Regge-Wheeler equation. Large- l solutions are found by applying a PN expansion ansatz to the Regge-Wheeler equation. Previous work has given ψ to 9.5PN order and to order e^2 (i.e., the near circular orbit limit). We calculate the expansion to 9PN but to e^{16} in eccentricity. It proves possible to find a few terms that have closed-form expressions, all of which are associated with logarithmic terms in the PN expansion. We also compare the numerical evaluation of our PN expansion to prior numerical calculations of ψ in close orbits to assess its radius of convergence. We find that the series is not as rapidly convergent as the one for the redshift invariant at $r \simeq 10M$ but still yielding $\sim 1\%$ accuracy for eccentricities $e \lesssim 0.25$.

PACS numbers: 04.25.dg, 04.30.-w, 04.25.Nx, 04.30.Db

I. INTRODUCTION

In a set of recent papers, we have presented high post-Newtonian (PN) order analytic expansions of black hole perturbation theory (BHPT) and gravitational self-force quantities at first order in the mass ratio $\varepsilon \ll 1$ for extreme-mass-ratio inspiral (EMRI) binaries in bound eccentric motion about a Schwarzschild black hole. In each case, these results are double expansions in PN order and in powers of the eccentricity e . This work included study in the dissipative sector of gravitational wave energy and angular momentum fluxes radiated to infinity [1–4] and fluxes radiated into the horizon [5] and study in the conservative sector of the redshift invariant [6]. The method involves using the Regge-Wheeler-Zerilli (RWZ) formalism [7, 8] and making analytic function expansions using the Mano-Suzuki-Takasugi (MST) formalism [9] and a general- l ansatz to find expansions of the mode functions. The metric perturbations and self-force are derived in the Regge-Wheeler (RW) gauge and mode-sum regularization is used. A sampling of other applications that have used this procedure include [10–16].

This paper applies those techniques to another gauge-invariant quantity, the spin-precession invariant. This invariant, ψ , quantifies the geodetic precession of a gyroscope attached to the smaller mass as it is parallel transported during its orbital motion. The test-body limit of the geodetic precession is well known. We are concerned with the first order in ε correction to ψ , $\Delta\psi$, induced by the small but finite mass of the secondary. For an eccentric orbit, ψ is defined as the fractional precessional angular advance Ψ , per azimuthal angular advance Φ , accumulated over one radial libration. The calculation of $\Delta\psi$ bears some similarities to that of the redshift invariant, as they both depend on the metric perturbation at the point mass location. As discussed in [6, 16], the

PN order of individual modes of the local metric perturbation do not increase with l , which means that the mode functions and metric perturbation must be calculated for arbitrarily high l . This general- l complication is handled by utilizing a PN-expansion ansatz solution to the RW equation valid for all l above the target PN order [6, 10–12, 14, 16].

Calculating $\Delta\psi$ presents new challenges. One is the need to calculate the (conservative) self-force itself. (In contrast, the redshift invariant only required the metric perturbation.) Calculation of all of the metric perturbation components and the components of the self-force is roughly an order of magnitude more computationally costly than the effort involved in finding the redshift invariant. Furthermore, the self-force is gauge dependent. Fortunately, the regularization is performed on the l -modes of the spin-precession invariant itself, extracting the gauge invariant result directly. However, the mode-sum regularization procedure in this case requires two regularization parameters in order for the mode-sum to converge.

The spin-precession invariant was originally calculated for circular orbits in [17], both numerically and as a full arbitrary-mass-ratio PN expansion to 3PN absolute order. (Note that in contrast to previous papers on fluxes, where we referred to relative PN orders, here we connote PN order with the power of the PN compactness parameter (y or $1/p$) appearing in the expansion of $\Delta\psi$, as is conventional in papers on the spin invariant.) The spin-precession invariant was previously found [14] to 21.5PN in the circular-orbit limit using BHPT analytic expansions. In the eccentric-orbit case, results were found both numerically and as a 3PN expansion in [18]. Note, that the circular-orbit quantity $\Delta\psi^{\text{circ}}$ is not the same as its eccentric-orbit counterpart $\Delta\psi^{\text{ecc}}$ when the latter is taken in the limit $e \rightarrow 0$. The eccentric-orbit definition

relies on angular changes accumulated over one radial libration. In the limit as $e \rightarrow 0$, apsidal advance becomes indistinguishable from azimuthal advance but the difference in these definitions involves the order ε correction to the apsidal advance. The calculation of the eccentric-orbit version was separately found [18] to 9.5PN. The $\mathcal{O}(e^2)$ correction was then computed to 3PN in [18], to 6PN in [19], to 9PN in [20], and then to 9.5PN in [21]. The present work finds $\Delta\psi$ to 9PN but takes the eccentricity expansion to e^{16} , breaking away from the nearly circular orbit limit.

Conservative quantities like the spin-precession invariant supply crucial terms in effective-one-body (EOB) potentials [13, 16, 19, 20, 22–27] and also contribute directly to the EMRI cumulative phase at post-1 adiabatic order [28]. A procedure is described by [19] for translating the expansion of $\Delta\psi$ to the EOB gyrogravitomagnetic potential $g_{S*}(1/r, p_r, p_\varphi)$, thus informing the spin-orbit sector of EOB dynamics. The spin-precession invariant expansion in this paper can be transcribed to EOB form to enhance further the knowledge of the spin-orbit part.

The structure of this paper is as follows: In Sec. II we briefly outline (i) the setup of the orbital motion problem, (ii) the MST formalism for computing solutions and PN expansions of specific l modes, (iii) the procedure for finding general- l parts of the expansion, and (iv) the calculation of the (local) metric perturbation. Sec. III (i) defines the spin-precession invariant, (ii) describes the background tetrad and how to calculate the precession, (iii) summarizes how the first-order correction to the spin precession is computed with a definition that is gauge invariant, and (iv) how mode-sum regularization is applied to the spin invariant. Then, the results of our calculations are presented in Sec. IV, first as a PN expansion in the compactness parameter $1/p$ and second as an expansion in the PN parameter y . Our expansions are also evaluated numerically at a pair of close orbital separations and compared to prior numerical calculations. Sec. V concludes with summary and outlook.

Throughout this paper we choose units such that $c = G = 1$, though $\eta = 1/c$ is briefly reintroduced for PN-expansion bookkeeping purposes. We use metric signature $(-+++)$. Our notation for the RWZ formalism follows that found in [3, 15], which in part derives from notational changes for tensor spherical harmonics and perturbation amplitudes made by Martel and Poisson [29]. For the MST formalism, we largely make use of the discussion and notation found in the review by Sasaki and Tagoshi [30].

II. FORMALISM FOR BLACK HOLE PERTURBATIONS AND POST-NEWTONIAN EXPANSIONS

A pair of recent papers [1, 6] outlined our approach to calculating the first-order metric perturbation for eccentric-orbit non-spinning EMRIs and PN expanding

regularized quantities. The more recent paper used the technique to derive the high-order PN expansion of the redshift invariant. For our present purpose, in calculating the spin-precession invariant, and to set the notation, we briefly recite in this section the calculational approach. See [1, 6] for further details.

A. Bound orbits and PN compactness parameters

The secondary is treated as a point mass μ in bound geodesic orbit about a Schwarzschild black hole of mass M , with $\varepsilon = \mu/M \ll 1$. We use Schwarzschild coordinates $x^\mu = (t, r, \theta, \varphi)$ that produce the line element

$$ds^2 = -f dt^2 + f^{-1} dr^2 + r^2 (d\theta^2 + \sin^2 \theta d\varphi^2), \quad (2.1)$$

with $f = 1 - 2M/r$. Restricting the motion to the equatorial plane, the four-velocity is

$$u^\alpha(\tau) = \frac{dx_p^\alpha(\tau)}{d\tau} = \left(\frac{\mathcal{E}}{f_p}, u^r, 0, \frac{\mathcal{L}}{r_p^2} \right), \quad (2.2)$$

where \mathcal{E} and \mathcal{L} , the specific energy and angular momentum, are constants of the motion and the subscript p indicates evaluation along the worldline of the particle. The orbital motion is reparameterized using Darwin's parameters (χ, p, e) [31–33], connected by

$$\begin{aligned} \mathcal{E}^2 &= \frac{(p-2)^2 - 4e^2}{p(p-3-e^2)}, \quad \mathcal{L}^2 = \frac{p^2 M^2}{p-3-e^2}, \\ r_p(\chi) &= \frac{pM}{1+e \cos \chi}. \end{aligned} \quad (2.3)$$

Here p is the semilatus rectum and its reciprocal $1/p$ serves as one choice for a PN compactness parameter. In the Darwin parameterization, one radial libration corresponds to 2π advance in χ . Motion in the other three coordinates, along with proper time τ , are found by integrating ordinary differential equations (ODEs) in χ [32, 34]. Most of these equations of motion can be initially PN expanded and then integrated analytically order by order. For example, the radial period is found from the following integral

$$T_r = \int_0^{2\pi} \frac{r_p(\chi)^2}{M(p-2-2e \cos \chi)} \left[\frac{(p-2)^2 - 4e^2}{p-6-2e \cos \chi} \right]^{1/2} d\chi,$$

and it is immediately clear how the integrand may be expanded in powers of $1/p$, resulting in a series of elementary trigonometric integrals. From that expansion then follows an expansion for the radial frequency, $\Omega_r = 2\pi/T_r$. In the case of azimuthal motion, the solution for $\varphi_p(\chi)$ can be obtained analytically prior to PN expansion

$$\Omega_\varphi = \frac{4}{T_r} \left(\frac{p}{p-6-2e} \right)^{1/2} K \left(-\frac{4e}{p-6-2e} \right), \quad (2.4)$$

where $K(m)$ is the complete elliptic integral of the first kind [35]. The solution can be readily PN expanded in $1/p$. Once the mean angular rate is known, the alternative standard PN compactness parameter $y = (M\Omega_\varphi)^{2/3}$ can be obtained in terms of $1/p$, and then inverted for $p(y)$. For eccentric motion, PN expansion in $1/p$ or y leads to related expansion in powers of eccentricity e .

B. Gravitational perturbations and analytic expansion of l -mode solutions

On a Schwarzschild background, we can obtain metric perturbations either via the Regge-Wheeler-Zerilli (RWZ) [7, 8] formalism (see recent uses [6, 16, 36]) or by use of the Bardeen-Press-Teukolsky equation and radiation gauge [19]. In this paper, we adhere to our previous RWZ approach, in which the RWZ master equations have the following form in the frequency domain (FD)

$$\left[\frac{d^2}{dr_*^2} + \omega^2 - V_l(r) \right] X_{lmn}(r) = Z_{lmn}(r). \quad (2.5)$$

Here $r_* = r + 2M \ln |r/2M - 1|$ is the tortoise coordinate, $\omega \equiv \omega_{mn} = m\Omega_\varphi + n\Omega_r$ are discrete frequencies from the

multiperiodic background geodesic motion, and the FD source term is

$$Z_{lmn} = \frac{1}{T_r} \int_0^{2\pi} (G_{lm}(t) \delta[r - r_p(t)] + F_{lm}(t) \delta'[r - r_p(t)]) e^{i\omega t} dt. \quad (2.6)$$

The source terms and potentials $V_l(r)$ are $(l+m)$ parity-dependent. The source terms can be found in [36].

The homogeneous version of the master equation yields two independent (causal) solutions. One, $X_{lmn}^{\text{in}} = X_{lmn}^-$, is a downgoing wave at the future horizon, while the other, $X_{lmn}^{\text{up}} = X_{lmn}^+$, is an outgoing wave at future null infinity. The odd-parity homogeneous (Regge-Wheeler) equation is more readily solved. For even parity cases of $l+m$, the Regge-Wheeler equation can be solved again and those solutions can be transformed to their even-parity counterparts using the Detweiler-Chandrasekhar transformation [37–40].

Once the homogeneous solutions are calculated (discussed below), the inhomogeneous solutions to (2.5) are found, which starts by computing the normalization coefficients

$$C_{lmn}^\pm = \frac{1}{W_{lmn} T_r} \int_0^{2\pi} \left(\frac{dt}{d\chi} \right) \left[\frac{1}{f_p} G_{lm}(\chi) X_{lmn}^\mp + \left(\frac{2M}{r_p^2 f_p^2} X_{lmn}^\mp - \frac{1}{f_p} \frac{dX_{lmn}^\mp}{dr} \right) F_{lm}(\chi) \right] e^{i\omega t(\chi)} d\chi, \quad (2.7)$$

where W_{lmn} is the Wronskian. The full time-domain solutions follow from applying the method of extended homogeneous solutions [41], using the combinations $C_{lmn}^+ X_{lmn}^+$ and $C_{lmn}^- X_{lmn}^-$ (see also [1, 36]).

As discussed in [1, 6], solutions for the modes of the master function (at least for small values of l) are determined using the MST formalism [9], with an expansion in analytic functions. The odd-parity MST solution for X_{lmn}^+ (up to arbitrary normalization) is

$$X_{lmn}^+ = e^{iz} z^{\nu+1} \left(1 - \frac{\epsilon}{z} \right)^{-i\epsilon} \sum_{j=-\infty}^{\infty} a_j (-2iz)^j \frac{\Gamma(j+\nu+1-i\epsilon)\Gamma(j+\nu-1-i\epsilon)}{\Gamma(j+\nu+3+i\epsilon)\Gamma(j+\nu+1+i\epsilon)} \times U(j+\nu+1-i\epsilon, 2j+2\nu+2, -2iz). \quad (2.8)$$

Here, ν is the renormalized angular momentum, defined to make the double-sided summation converge, and U is the irregular confluent hypergeometric function. Other quantities are $\epsilon = 2M\omega\eta^3$, $z = r\omega\eta$, with $\eta = 1/c$ being a reintroduced PN parameter. To obtain a solution, ν and a_j are ascertained through a continued fraction calculation [9, 30], which in our application also then leads to series in ϵ for both. PN expansions of the other terms in (2.8) then follow, with the result expressible in series in both z and ϵ .

The downgoing (or in) solutions X_{lmn}^- have similar function expansion

$$X_{lmn}^- = e^{-iz} \left(\frac{z}{\epsilon} - 1 \right)^{-i\epsilon} \left(\frac{\epsilon}{z} \right)^{i\epsilon+1} \sum_{j=-\infty}^{\infty} a_j \frac{\Gamma(j+\nu-1-i\epsilon)\Gamma(-j-\nu-2-i\epsilon)}{\Gamma(1-2i\epsilon)} \times {}_2F_1(j+\nu-1-i\epsilon, -j-\nu-2-i\epsilon; 1-2i\epsilon; 1-z/\epsilon), \quad (2.9)$$

with ν and a_j here being identical to those in (2.8) (up to overall normalization of the latter). The process of expanding these homogeneous solutions by collecting on powers of η is fully described in [1], based on the methods presented in [14]. As described in [6, 14], z -independent factors are removed from these solutions to reduce their complexity, since such factors eventually cancel through appearance in the Wronskian.

As discussed in [1, 6, 10, 14], in conservative sector calculations mode-sum regularization requires summing perturbations over all l . This necessitates an alternative approach of directly PN-expanding the homogeneous version of the master equation (2.5) for general l . As shown in [10, 14], the PN-expansion ansatz for solving the RW equation is

$$\begin{aligned} X_{lmn}^+ &= (z)^{-\nu} (1 + A_2 \eta^2 + A_4 \eta^4 + \cdots + A_{2l} \eta^{2l} + \mathcal{O}(\eta^{2l+1})), \\ X_{lmn}^- &= \left(\frac{\epsilon}{z}\right)^{-\nu-1} (1 + B_2 \eta^2 + B_4 \eta^4 + \cdots + B_{2l} \eta^{2l} + \mathcal{O}(\eta^{2l+1})), \end{aligned} \quad (2.10)$$

where the A_i and B_i are functions of z, ϵ, l . The ansatz breaks down at PN orders at and above $\mathcal{O}(\eta^{2l})$. If a target PN order P is set, the ansatz will be useless for $l \leq P$. For those finite number of modes, the MST formalism is used instead. Once ν is found by PN-expanding the continued fraction calculation, the homogeneous RW equation becomes

$$\left[\left(1 - \frac{\epsilon}{z}\right) \frac{\partial}{\partial z} \left(\left(1 - \frac{\epsilon}{z}\right) \frac{\partial}{\partial z} \right) + \eta^2 + \left(1 - \frac{\epsilon}{z}\right) \left(\frac{l(l+1)}{z^2} - \frac{3\epsilon}{z^3} \right) \eta^2 \right] X_{lmn}^\pm = 0. \quad (2.11)$$

The ODE is then solved order by order. Even-parity homogeneous solutions are again found using the Detweiler-Chandrasekhar transformation.

As previously noted [6], the expansion of the even-parity normalization integral is the bottleneck in the calculation, requiring for example ~ 7 days and 20GB of memory on the UNC supercomputing cluster Longleaf to reach 10PN and e^{20} relative order. Furthermore, two relative PN orders and three orders in e are lost in constructing and regularizing the spin-precession invariant. Thus, our expansion is restricted to 9PN (8PN relative order) and e^{16} .

C. Metric perturbation l -modes and non-radiative modes

Since we use RWZ gauge, calculation of the l -modes of the metric perturbation (locally) follows the procedure discussed in Section II of [6] (see also earlier work [16, 36]). Briefly, the metric components as functions of χ are

$$\begin{aligned} p_{rr}^l(\chi) &= \left(\frac{d\chi}{dr}\right) \sum_{mn} \frac{Y_{lm}(\pi/2, 0)}{f} C_{lmn}^\pm e^{im\varphi - i\omega t} \left\{ \left[\left(\frac{dr}{d\chi}\right) \frac{\Lambda(\lambda+1)}{fr} - \left(\frac{dr}{d\chi}\right) \frac{\Lambda}{f} A(\chi) + r \left(\frac{dA(\chi)}{d\chi}\right) \right] X_{lmn}^\pm(\chi) \right. \\ &\quad \left. + (rA(\chi) - \Lambda) \left(\frac{dX_{lmn}^\pm(\chi)}{d\chi}\right) + r \frac{d}{d\chi} \left[f \left(\frac{d\chi}{dr}\right) \left(\frac{dX_{lmn}^\pm(\chi)}{d\chi}\right) \right] \right\}, \\ p_{tr}^l(\chi) &= \sum_{mn} Y_{lm}(\pi/2, 0) C_{lmn}^\pm e^{im\varphi - i\omega t} (-i\omega) \left[r \left(\frac{d\chi}{dr}\right) \left(\frac{dX_{lmn}^\pm(\chi)}{d\chi}\right) + rB(\chi) X_{lmn}^\pm(\chi) \right], \\ p_{tt}^l(\chi) &= f^2 p_{rr}^{l,\pm}, \\ p_{AB}^l(\chi) &= r^2 \Omega_{AB} \sum_{mn} Y_{lm}(\pi/2, 0) C_{lmn}^\pm e^{im\varphi - i\omega t} \left[f \left(\frac{d\chi}{dr}\right) \partial_\chi X_{lmn}^{e,\pm} + A(\chi) X_{lmn}^{e,\pm} \right], \\ p_{tB}^l(\chi) &= \left(\frac{f}{2}\right) \sum_{mn} X_B^{lm}(\pi/2, 0) C_{lmn}^\pm e^{im\varphi - i\omega t} \left(\frac{d\chi}{dr}\right) \frac{d}{d\chi} (r X_{lmn}^\pm), \\ p_{rB}^l(\chi) &= \left(\frac{r}{2f}\right) \sum_{mn} X_B^{lm}(\pi/2, 0) C_{lmn}^\pm e^{im\varphi - i\omega t} (-i\omega) X_{lmn}^\pm, \end{aligned} \quad (2.12)$$

with

$$\begin{aligned} \lambda &= \frac{1}{2}(l+2)(l-1), & \Lambda &= \lambda + \frac{3M}{r}, \\ A(r) &= \frac{1}{r\Lambda} \left[\lambda(\lambda+1) + \frac{3M}{r} \left(\lambda + \frac{2M}{r} \right) \right], \\ B(r) &= \frac{1}{rf\Lambda} \left[\lambda \left(1 - \frac{3M}{r} \right) - \frac{3M^2}{r^2} \right]. \end{aligned} \quad (2.13)$$

The up (+) or in (−) mode functions are used depending

upon which side in r of the point mass the evaluation is taken. The perturbation l -modes (once sums over m are made) are continuous, but C^0 , at the particle location. Sums over m involve application of the addition theorem for spherical harmonics. In [6] we discuss the most efficient way of calculating PN expansions of the resulting sums over m (see Section IID of that paper). The spin-precession invariant is calculated from the local

self-force, which involves the metric perturbation and its derivatives. Expressions for the derivatives can be easily derived from (2.12). The l -modes of the metric perturbation derivatives are discontinuous across the particle location, a fact that is important in the regularization of the spin-precession invariant.

Another aspect of computing the self-force is that, in applying a derivative with respect to χ , an expansion over powers of eccentricity will lose an order in e . Moreover, the eccentricity expansions lose a total of 3 orders in e in moving from the self-force to the spin invariant. The computation of high-order series in e is the most consuming part of the construction of the metric perturbations, particularly initially in the case of general l . However, added investigation showed that this difficulty can be avoided in the latter case by observing that the general- l metric perturbations yield finite polynomials in e on an individual PN-order basis. These polynomials increase in degree linearly with PN order. Once this pattern was recognized, PN terms in the general- l expansion could be determined in closed form with only a low-order (imbedded) polynomial in eccentricity. The computational bottleneck was then transferred to the specific- l part of the calculation, which does not simplify in the same fashion. The resulting change in the technique allowed the spin-precession invariant to be computed to much higher order in eccentricity at lower PN orders. For example, it allowed us to determine the 4PN function $\Delta\psi_4$ to e^{30} .

Finally, to complete the metric perturbation and self-force calculation, the radiative modes must be augmented to include the nonradiative $l = 0$ and $l = 1$ modes, originally found by Zerilli [8] but gauge transformed [42] to maintain asymptotic flatness. We listed those modes in our previous paper [6], and they are described more fully in [16] and in earlier papers cited therein.

III. PROCEDURE FOR CALCULATING THE SPIN-PRECESSION INVARIANT

A. Overview

The smaller body is assumed to be endowed with a spin s_α , which undergoes precession during the orbital motion about the heavier mass. The spin is parallel transported $Ds_\alpha/d\tau = 0$ along the geodesic with its tangent vector u^α , and the spin maintains its orthogonality $s_\alpha u^\alpha = 0$ and the constancy of its norm $s_\alpha s^\alpha$. This spin-orbit, or geodetic, precession has a nonzero rate of advance in the test-body limit ($\mu = 0$) and a self-force correction at first order in the mass ratio ε and beyond. We seek to calculate the first-order correction to the precession in bound eccentric orbits about a nonspinning (Schwarzschild) primary (thus eliminating consideration of Lense-Thirring precession). Our presentation follows that of [17–19], which we summarize in this section.

The spin-precession invariant for eccentric orbits is a generalization given by [18] of the definition used for cir-

cular orbits [17]. An invariant ψ is defined via a ratio that involves the accumulated azimuthal phase Φ and the accumulated precession of the spin vector Ψ over one radial libration period T_r . Explicitly, the quantity is given by

$$\psi = 1 - \frac{\Psi}{\Phi}. \quad (3.1)$$

This scalar is a function of the mass ratio ε (i.e., subject to self-force correction $\Delta\psi$) and orbital parameters. The latter are best chosen as the observable frequencies Ω_r and Ω_φ , lending the definition of ψ a gauge invariant character. This procedure is directly analogous to that in constructing the redshift invariant [6], where the frequencies were held fixed through first order in the mass ratio. Since $\Phi = \Omega_\varphi T_r$ will itself be fixed, only the self-force correction $\Delta\Psi$ need be computed.

The invariant ψ encodes a portion of the first-order conservative dynamics, giving it relevance to the creation of waveform templates for LISA. How ψ can be transcribed to the EOB gyrogravitomagnetic ratio quantity $g_{S*}(1/r, p_r, p_\varphi)$, which partially characterizes the spin-orbit sector of the EOB Hamiltonian, was mapped out in [19]. The expansion of ψ helps describe the case where the smaller body is (weakly) spinning.

B. Spin precession and background reference frame

The behavior of Ψ is found by computing the parallel transport of s_α along a geodesic of the perturbed (regularized) metric. To facilitate the calculation, a reference frame tetrad e_a^α is introduced (here α is the spacetime index and a indicates the frame element). Then, the spin components in the frame precess [18] according to

$$\begin{aligned} \frac{ds}{d\tau} &= \mathbf{w} \times \mathbf{s}, \\ (\mathbf{s})_i &= e_i^\alpha s_\alpha, \\ (\mathbf{w})_i &= -\frac{1}{2}\epsilon_{ijk}w^{jk}, \\ w_{ij} &= -g_{\alpha\beta}e_i^\alpha \frac{De_j^\beta}{d\tau}. \end{aligned} \quad (3.2)$$

The precessional angular velocity components use the base symbol w instead of ω to avoid confusion with the discrete frequency spectrum ω_{mn} of the gravitational perturbations. The angular velocity is subject to the choice made for the reference frame.

A suitable frame in the background ($\mu \rightarrow 0$ limit) was given by Marck [43] (see also [18, 19], as well as [44] for a different application), aligned with one leg perpendicular to the orbital (equatorial) plane and another directed along the line with the primary

$$\begin{aligned} e_0^\mu &= u^\mu = \left(\frac{\mathcal{E}}{f}, u^r, 0, \frac{\mathcal{L}}{r^2} \right), \\ e_1^\mu &= \frac{1}{f\sqrt{1 + \mathcal{L}^2/r^2}}(u^r, f\mathcal{E}, 0, 0), \end{aligned}$$

$$e_2^\mu = (0, 0, 1/r, 0),$$

$$e_3^\mu = \frac{1}{r\sqrt{1 + \mathcal{L}^2/r^2}} \left(\frac{\mathcal{E}\mathcal{L}}{f}, \mathcal{L}u^r, 0, 1 + \frac{\mathcal{L}^2}{r^2} \right). \quad (3.3)$$

This polar alignment can be maintained when $\mu \neq 0$. The frame is non-inertial and a gyroscope will appear to precess with frequency $\dot{\Psi} = w_{13}$. (The precession can also be found by making a $U(1)$ transformation [44] in the equatorial plane to an inertial frame.) At lowest order the (background) geodetic angular rate is

$$w_{13}^{(0)} = \frac{\mathcal{E}\mathcal{L}}{r^2 + \mathcal{L}^2}. \quad (3.4)$$

C. Spin precession and self-force in the perturbed frame

The accumulated phase of the spin precession is then

$$\Psi = \oint w_{13}(\tau) d\tau = \Psi_0 + \Delta\Psi, \quad (3.5)$$

with the integral taken over one period of radial motion. The last part of the expression splits Ψ into 0th and 1st order components, with $\Delta\Psi$ being the first-order (conservative) correction we seek. Here, $\Delta\Psi$ refers to the perturbation measured when the orbital frequencies have been held constant.

The procedure to compute $\Delta\Psi$ is established in [18–20]. Assuming that $\delta\Psi$ is a correction calculated without holding the orbital frequencies fixed, $\Delta\Psi$ is recovered by subtracting off perturbations in the frequencies

$$\Delta\Psi = \delta\Psi - \frac{\partial\Psi_0}{\partial\Omega_r} \delta\Omega_r - \frac{\partial\Psi_0}{\partial\Omega_\varphi} \delta\Omega_\varphi. \quad (3.6)$$

An alternative calculation uses first-order changes in T_r and Φ [18]

$$\Delta\Psi = \delta\Psi - \frac{\partial\Psi_0}{\partial T_r} \delta T_r - \frac{\partial\Psi_0}{\partial\Phi} \delta\Phi, \quad (3.7)$$

which we found more computationally convenient. Note that henceforth, except for our use of Ψ_0 and $w_{13}^{(0)}$, lowest-order quantities will simply be denoted by their plain base symbol, while most first-order corrections will explicitly carry a δ (perturbed frequencies) or Δ (fixed frequencies) prefix. The exception is the metric perturbation $p_{\mu\nu}$, where the notation already indicates a first-order quantity.

At first order, the integral for Ψ experiences a change due to corrections in both w_{13} and τ . The result is [18, 45]

$$\delta\Psi = \int_0^{2\pi} \left(\frac{\delta w_{13}}{w_{13}} - \frac{\delta u^r}{u^r} \right) w_{13} \frac{d\tau}{d\chi} d\chi. \quad (3.8)$$

The correction to w_{13} can be found [18, 19] via expansion of its definition

$$\delta w_{13} = \frac{1}{2} w_{13} p_{\mu\nu} e_0^\mu e_0^\nu + \delta\Gamma_{[31]0} + (c_{01} e_1^\mu + c_{03} e_3^\mu) e_{\nu[3} \nabla_\mu e_{1]}^\nu. \quad (3.9)$$

In deriving the expression above, a total derivative ($d/d\tau$) term has been neglected. The first term is proportional to the p_{00} tetrad projection of the metric perturbation (not p_{tt}) and the second term is the tetrad projection of the correction to the affine connection

$$\delta\Gamma_{[31]0} = (\delta\Gamma_{\mu\nu\beta} - p_{\mu\lambda} \Gamma_{\nu\beta}^\lambda) e_{[3}^\mu e_{1]}^\nu u^\beta. \quad (3.10)$$

The third term involves coefficients c_{01} and c_{03} that come from the variation of the tetrad

$$c_{01} = \frac{1}{f\sqrt{1 + \mathcal{L}^2/r^2}} (\mathcal{E}\delta u_{BS}^r - u^r \delta\mathcal{E}_{BS}), \quad (3.11)$$

$$c_{03} = \frac{\delta\mathcal{L}_{BS}}{r\sqrt{1 + \mathcal{L}^2/r^2}}. \quad (3.12)$$

Within these latter coefficients are terms, $\delta\mathcal{E}_{BS}$ and $\delta\mathcal{L}_{BS}$, that are χ -dependent conservative corrections to the (specific) energy and angular momentum defined by Barack and Sago [45]

$$\delta\mathcal{E}_{BS}(\chi) = \delta\mathcal{E}_{BS}(0) - \int_0^\chi F_t^{\text{cons}} \frac{d\tau}{d\chi'} d\chi', \quad (3.13)$$

$$\delta\mathcal{L}_{BS}(\chi) = \delta\mathcal{L}_{BS}(0) + \int_0^\chi F_\varphi^{\text{cons}} \frac{d\tau}{d\chi'} d\chi'. \quad (3.14)$$

The first term (integration constant) in each of these equations is the shift that occurs at periastron. These are explicitly shown [45] to be

$$\delta\mathcal{E}_{BS}(0) = \frac{(1+e)^2(p-2-2e)}{4e(p-3-e^2)} \left[\frac{(1-e)^2(p-2+2e)}{Mp^{3/2}\sqrt{(p-2)^2-4e^2}} \int_0^\pi F_\varphi^{\text{cons}} \frac{d\tau}{d\chi} d\chi + \int_0^\pi F_t^{\text{cons}} \frac{d\tau}{d\chi} d\chi \right], \quad (3.15)$$

$$\delta\mathcal{L}_{BS}(0) = \frac{Mp^{3/2}\sqrt{(p-2)^2-4e^2}}{4e(p-3-e^2)} \left[\frac{(1-e)^2(p-2+2e)}{Mp^{3/2}\sqrt{(p-2)^2-4e^2}} \int_0^\pi F_\varphi^{\text{cons}} \frac{d\tau}{d\chi} d\chi + \int_0^\pi F_t^{\text{cons}} \frac{d\tau}{d\chi} d\chi \right]. \quad (3.16)$$

Lastly, δu_{BS}^r is the first-order correction to the radial velocity. It can be derived from the normalization of the four-velocity condition (in the background spacetime [45]), which leads to $\mathcal{E}\delta\mathcal{E}_{BS} - u^r\delta u_{BS}^r - r^{-2}f\mathcal{L}\delta\mathcal{L}_{BS} = 0$ and from there to

$$\delta u_{BS}^r = \frac{\mathcal{E}}{u^r}\delta\mathcal{E}_{BS} - \frac{f}{r^2u^r}\mathcal{L}\delta\mathcal{L}_{BS}. \quad (3.17)$$

As usual, the conservative part of the self-force, F_μ^{cons} , is given [45] by the symmetric combination

$$F_\mu^{\text{cons}} = \frac{1}{2} \left(F_\mu(\chi) + \epsilon^{(\mu)} F_\mu(-\chi) \right), \quad (3.18)$$

where $\epsilon^{(\mu)} = (-1, 1, 1, -1)$. Using the retarded self-force in the expression above yields a singular result at the

particle location. Instead, the regularized self-force can be found using the regular metric perturbation $p_{\mu\nu}^R$ in

$$F_R^\alpha = \frac{1}{2} (g^{\alpha\delta}u^\beta - 2g^{\alpha\beta}u^\delta - u^\alpha u^\beta u^\delta) u^\gamma \nabla_\delta p_{\beta\gamma}^R. \quad (3.19)$$

However, since we are concerned with computing a single scalar invariant, it is simpler to work instead with the full, unregularized self-force, decomposed into l -modes. This leads to an l -mode decomposition of the (unregularized) spin invariant correction, with modes $\Delta\psi^l$. We then apply mode-sum regularization directly to the spin-precession invariant.

Hence, with the l -modes of the retarded metric perturbation and self-force available, it is straightforward to evaluate \mathcal{E}_{BS}^l , \mathcal{L}_{BS}^l , and $\Gamma_{[31]0}^l$. The rest of the calculation for $\delta\Psi^l$ is then condensed [20] to the following integral

$$\delta\Psi^l = \int_0^{2\pi} \left[\delta\Gamma_{[31]0}^l + \left(\frac{(r^2 + \mathcal{L}^2)(3M-r)\mathcal{L}}{r^5(u^r)^2} - \frac{\mathcal{L}}{r^2} \right) \delta\mathcal{E}_{BS}^l + \left(\frac{\mathcal{E}}{r^2} - \frac{\mathcal{E}\mathcal{L}^2(3M-r)}{r^5(u^r)^2} \right) \delta\mathcal{L}_{BS}^l \right] \frac{d\tau}{d\chi} d\chi. \quad (3.20)$$

Then, $\Delta\Psi^l$ can be determined from $\delta\Psi^l$ by removal of the frequency corrections, which involves use of the following formulas [18, 20]

$$\delta T_r^l = \int_0^{2\pi} \left(\frac{\delta\mathcal{E}_{BS}^l}{\mathcal{E}} - \frac{\delta(u_{BS}^r)^l}{u^r} \right) \frac{\mathcal{E}}{f} \frac{d\tau}{d\chi} d\chi, \quad (3.21)$$

$$\delta\Phi^l = \int_0^{2\pi} \left(\frac{\delta\mathcal{L}_{BS}^l}{\mathcal{L}} - \frac{\delta(u_{BS}^r)^l}{u^r} \right) \frac{\mathcal{L}}{r^2} \frac{d\tau}{d\chi} d\chi. \quad (3.22)$$

D. PN and eccentricity expansion issues

Even though we have not belabored the process, each step in this procedure involves calculating an analytic PN expansion using MATHEMATICA. (Illustrative short expansions of various intermediate quantities in the procedure can be found in Section III of [19].) Given eccentric orbital motion, the PN expansion necessarily involves an expansion in powers of eccentricity e as well. We have sought to go as deeply as possible in PN order and (especially) eccentricity order. High-order expansion in eccentricity opens up the possibility of finding eccentricity-dependent terms that have closed-form expressions or infinite series with analytically-known coefficient sequences [2, 4, 6].

We restate for emphasis one issue with calculating the PN and eccentricity expansions of the spin-precession in-

variant. As we have discussed, the procedure begins with calculating the mode functions X_{lmn}^\pm and their normalizations C_{lmn}^\pm . Assume that C_{lmn}^+ , for example, has been calculated in the general- l case to a relative PN order of \mathcal{P} and to order $e^{2\mathcal{N}}$ in eccentricity. We find that once derivatives have been taken, to calculate the metric perturbation and the self-force, and the various projections have been made, the expansion of the spin-precession invariant has lost two relative orders in \mathcal{P} and two orders in e^2 (i.e., two order in \mathcal{N}). For example, if C_{lmn}^+ were known in the general- l case to 8PN (relative) and e^{20} , the computation of the general- l contribution to the spin invariant is limited to 6PN relative order (7PN absolute order, as it is conventionally defined) and e^{16} . One caveat, however, is that the general- l expansion does not contribute to the spin precession at half-integer orders. Thus, as long as the specific- l contributions are appropriately extended, the final result in this example would be an expansion for ψ that reaches 7.5PN (absolute) and e^{16} .

E. Regularization

The final step in the procedure is regularization. As mentioned in Sec. IIIC, instead of regularizing the self-force itself, we calculate l -modes of the spin invariant

using l -modes of the unregularized retarded self-force. Then, we make a mode-sum regularization of the spin invariant itself, in a procedure that is similar to but slightly more involved than the way in which we previously regularized the redshift invariant [6]. Because the spin invariant involves derivatives of the metric perturbation, l -mode contributions to the singular behavior grow like l . Mode-sum regularization requires subtracting off terms from the expansion of the singular field

$$\Delta\psi = \sum_{l=0}^{\infty} \left(\Delta\psi_{\text{ret}}^{l,\pm} \mp A_S(2l+1) - B_S \right). \quad (3.23)$$

The calculation on the right is direction dependent, based on whether the particle location is approached from outside or inside of r_p , but yields the same final value. The coefficients, A_S and B_S , are the two regularization parameters required to allow the sum to converge. However, usually regularization parameters are defined by decomposing every vector and tensor component into a sum over scalar spherical harmonics. Then, each regularization parameter is l independent. In the present application, our l is different and refers to the tensor spherical harmonic index, with the implication [46] that A_S at least is not completely independent of l but changes value for $l = 0$ and $l = 1$. Furthermore, neither A_S nor B_S are

known a priori.

The workaround for the latter issue involves using the general- l expansion. Because A_S and B_S must match the large- l behavior of $\Delta\psi^{l,\text{ret}}$, we can expand our general- l result for $\Delta\psi_{\text{ret}}^l$ about $l = \infty$ to find two coefficients, A_∞ and B_∞ . Then theoretically, $B_\infty = B_S$ (for all l) and $A_\infty = A_S$ for $l \geq 2$. The qualification is that regularization and decomposition of the singular field is usually discussed in the context of Lorenz gauge [47]. While we are working in a different gauge, mode-sum regularization carries across [48] to select other gauges, with RWZ gauge [49] being one.

The remaining problem is the behavior of A_S when $l = 0, 1$. The solution is to recognize that A_S flips sign across the location of the point mass [46] (see (2.12)), allowing (3.23) to be replaced by [19, 20]

$$\Delta\psi = \sum_{l=0}^{\infty} \left(\frac{1}{2} (\Delta\psi_{\text{ret}}^{l,+} + \Delta\psi_{\text{ret}}^{l,-}) - B_\infty \right). \quad (3.24)$$

However, there is no reason to use (3.24) for every l . We can instead use (3.23) for all $l \geq 2$ and reserve use of (3.24) for only the $l = 0$ and $l = 1$ modes. The net effect is to reduce the calculation by roughly 50%.

IV. PN EXPANSIONS OF THE SPIN-PRECESSION INVARIANT

The procedure in the previous two sections was utilized to compute the spin-precession invariant expansion to 9PN order and to e^{16} in eccentricity. We present the expansions in this section using both $1/p$ and y as compactness parameters. The expansions are given in this paper to 8PN order, with the full series being available in electronic form at the Black Hole Perturbation Toolkit [50] website and at our research group website [51].

A. Spin-precession invariant as an expansion in $1/p$

Previous work in the circular-orbit limit has revealed [18] the general PN structure of $\Delta\psi$ to 9.5PN order. Expressed in terms of the compactness parameter $1/p$, the form of the expansion is

$$\begin{aligned} \Delta\psi = & \frac{\Delta\psi_1^p}{p} + \frac{\Delta\psi_2^p}{p^2} + \frac{\Delta\psi_3^p}{p^3} + (\Delta\psi_4^p + \Delta\psi_{4L}^p \log p) \frac{1}{p^4} + (\Delta\psi_5^p + \Delta\psi_{5L}^p \log p) \frac{1}{p^5} + \frac{\Delta\psi_{11/2}^p}{p^{11/2}} \\ & + (\Delta\psi_6^p + \Delta\psi_{6L}^p \log p) \frac{1}{p^6} + \frac{\Delta\psi_{13/2}^p}{p^{13/2}} + (\Delta\psi_7^p + \Delta\psi_{7L}^p \log p + \Delta\psi_{7L2}^p \log^2 p) \frac{1}{p^7} + \frac{\Delta\psi_{15/2}^p}{p^{15/2}} \\ & + (\Delta\psi_8^p + \Delta\psi_{8L}^p \log p + \Delta\psi_{8L2}^p \log^2 p) \frac{1}{p^8} + \left(\Delta\psi_{17/2}^p + \Delta\psi_{17/2L}^p \log p \right) \frac{1}{p^{17/2}} \\ & + (\Delta\psi_9^p + \Delta\psi_{9L}^p \log p + \Delta\psi_{9L2}^p \log^2 p) \frac{1}{p^9} + \dots \end{aligned} \quad (4.1)$$

Because this is a first-order self-force result, the entire right hand side should be viewed as multiplied by a factor of μ/M . For eccentric orbits, each of the quantities $\Delta\psi_k^p$, for different k , is no longer just a number but rather a function of the eccentricity e . The purpose of this section is to show the form of these functions.

In discussing energy and angular momentum fluxes (see e.g., [3]) it is conventional to factor out the circular-orbit limit with p^{-5} and refer to terms in the expansion by their relative PN order. Thus, the Peters-Mathews flux is 0PN

relative. In the spin-precession invariant expansion, the leading-order term is p^{-1} and we will refer to this as the 1PN (absolute) term. In our nomenclature, a k PN term is one that is proportional to p^{-k} .

The first three functions were all found previously [18] and shown to have closed forms

$$\Delta\psi_1^p = -1, \quad (4.2)$$

$$\Delta\psi_2^p = \frac{9 + 4e^2}{4}, \quad (4.3)$$

$$\Delta\psi_3^p = \left(\frac{739}{16} - \frac{123\pi^2}{64}\right) + e^2 \left(\frac{341}{16} - \frac{123\pi^2}{256}\right) - \frac{e^4}{2}. \quad (4.4)$$

Beyond 3PN order, only the circular-orbit behavior [18] and first term, e^2 , in eccentricity were known previously. The e^2 terms through 6PN had been calculated by [19] and [20] had found the e^2 behavior through 9PN. Our present work extends every term through 9PN order to e^{16} in eccentricity, allowing key parts of the functions $\Delta\psi_k^p(e)$ to be isolated in many cases and allowing us to find in a few cases complete, closed-form expressions.

The 4PN term is a case in which having enough terms in the eccentricity expansion allows us to identify elemental parts of the eccentricity functions. The behavior of the 4PN spin-precession invariant is reminiscent of the 3PN energy flux. We find first that the 4PN log term has a closed-form expression. Then, that same function reappears in the 4PN non-log term. It is then possible to see a grouping, as a series, that contains all of the log-transcendental numbers (which we denote by $\Delta\psi_4^{p,\chi}$ in analogy to similar functions in the energy flux, angular momentum flux, and redshift invariant expansions). We display $\Delta\psi_4^{p,\chi}$ in this paper to e^{16} . The remaining part of the 4PN non-log term is a polynomial on the appearance of π^2 and a remaining rational-number series. That latter rational-number series is also displayed here to e^{16} . The breakdown of the 4PN term is as follows:

$$\begin{aligned} \Delta\psi_4^p = & \left(-\frac{587831}{2880} - \frac{37961e^2}{160} - \frac{28129e^4}{480} - \frac{19015e^6}{1152} - \frac{138247e^8}{15360} - \frac{12431e^{10}}{2048} \right. \\ & \left. - \frac{327985e^{12}}{73728} - \frac{56393e^{14}}{16384} - \frac{725137e^{16}}{262144} + \dots \right) + \pi^2 \left(\frac{31697}{6144} - \frac{23729e^2}{4096} - \frac{23761e^4}{16384} \right) \\ & - 2 \left[\gamma_E + \log \left(\frac{8(1-e^2)^{3/2}}{1+\sqrt{1-e^2}} \right) \right] \Delta\psi_{4L}^p + \Delta\psi_4^{p,\chi}, \end{aligned} \quad (4.5)$$

$$\begin{aligned} \Delta\psi_4^{p,\chi} = & \left(-\frac{2216 \log(2)}{15} + \frac{729 \log(3)}{5} \right) + \left(\frac{55384 \log(2)}{15} - \frac{10206 \log(3)}{5} \right) e^2 + \left(-\frac{205917 \log(2)}{5} + \right. \\ & \left. \frac{3620943 \log(3)}{320} + \frac{1953125 \log(5)}{192} \right) e^4 + \left(\frac{11518508 \log(2)}{45} + \frac{3995649 \log(3)}{320} - \frac{68359375 \log(5)}{576} \right) e^6 \\ & + \left(-\frac{1597223897 \log(2)}{1350} - \frac{199689627159 \log(3)}{409600} + \frac{274244140625 \log(5)}{442368} + \frac{678223072849 \log(7)}{3686400} \right) e^8 \\ & + \left(\frac{27567693977 \log(2)}{4500} + \frac{1474172887599 \log(3)}{512000} - \frac{71310546875 \log(5)}{36864} - \frac{678223072849 \log(7)}{307200} \right) e^{10} \\ & + \left(-\frac{39584616236117 \log(2)}{1134000} - \frac{2523359744732097 \log(3)}{458752000} + \frac{1806540009765625 \log(5)}{445906944} \right. \\ & \left. + \frac{77643655602826369 \log(7)}{6370099200} \right) e^{12} + \left(\frac{7796904819020377 \log(2)}{47628000} - \frac{96876093468033783 \log(3)}{3211264000} \right. \\ & \left. - \frac{173056322265625 \log(5)}{3121348608} - \frac{1313351173426101691 \log(7)}{31850496000} \right) e^{14} + \left(-\frac{1349495913968063023 \log(2)}{2286144000} \right. \\ & \left. + \frac{44537688184006902231 \log(3)}{164416716800} - \frac{131695624109951171875 \log(5)}{1826434842624} \right. \\ & \left. + \frac{9397785802951526436547 \log(7)}{97844723712000} + \frac{81402749386839761113321 \log(11)}{4794391461888000} \right) e^{16} + \dots, \end{aligned} \quad (4.6)$$

$$\Delta\psi_{4L}^p = - \left(\frac{628}{15} + \frac{268e^2}{5} + \frac{37e^4}{10} \right). \quad (4.7)$$

Our result for the 4PN term is exceptional in one regard. As mentioned in Sec. II C, we are able to exploit a feature in the eccentricity expansion of the general- l part of the metric perturbation. At any given PN order, the eccentricity expansion of the general- l modes truncates at some power, which depends upon metric component and PN order

but not l . The only contributions to higher powers of e beyond this truncation point come from the (MST-derived) specific- l calculation. We used this feature to calculate the 4PN term to much higher order in eccentricity (e^{30} !). The resulting eccentricity series gave us another opportunity to look for additional closed-form expressions and infinite series with analytically recognizable coefficient sequences. While no additional such functions were identified, we are providing the full 4PN term to e^{30} in the online repositories [50, 51].

The breakdown of the 5PN term is similar. Once again, we have enough information in the lengthy eccentricity expansion to see that the 5PN log term is a polynomial. The 5PN log term reappears in the 5PN non-log term. There is then a χ -like grouping of terms that can be isolated in the 5PN non-log function. There is a closed-form expression identifiable that multiplies π^2 and the remainder is a rational-number series.

$$\Delta\psi_5^p = \left(-\frac{48221551}{19200} - \frac{948244847e^2}{403200} + \frac{213024509e^4}{134400} + \frac{6416801e^6}{19200} + \frac{21598637e^8}{161280} + \frac{61987887e^{10}}{716800} \right. \\ \left. + \frac{2519343e^{12}}{40960} + \frac{482228861e^{14}}{10321920} + \frac{25511929e^{16}}{688128} + \dots \right) + \pi^2 \left(\frac{2483157}{8192} + \frac{21274445e^2}{49152} \right) \quad (4.8)$$

$$\Delta\psi_5^{p,\chi} = \left(\frac{155894 \log(2)}{105} - \frac{31347 \log(3)}{28} \right) + \left(-\frac{4518706 \log(2)}{105} + \frac{4430133 \log(3)}{320} + \frac{9765625 \log(5)}{1344} \right) e^2 \\ + \left(\frac{103760293 \log(2)}{180} - \frac{31627665 \log(3)}{1792} - \frac{3850703125 \log(5)}{16128} \right) e^4 + \left(-\frac{7257966409 \log(2)}{1512} - \frac{412866263889 \log(3)}{286720} + \frac{185751484375 \log(5)}{73728} + \frac{96889010407 \log(7)}{221184} \right) e^6 \\ + \left(\frac{1363049747783 \log(2)}{37800} + \frac{193316307253281 \log(3)}{11468800} - \frac{179678368984375 \log(5)}{12386304} - \frac{458460436354739 \log(7)}{44236800} \right) e^8 \\ + \left(-\frac{12831673840577 \log(2)}{45360} - \frac{7224124751440749 \log(3)}{91750400} + \frac{8043417607578125 \log(5)}{148635648} + \frac{355523097835854137 \log(7)}{3538944000} \right) e^{10} \\ + \left(\frac{183330830280580517 \log(2)}{95256000} - \frac{805502573948046501 \log(3)}{12845056000} - \frac{422974129832265625 \log(5)}{4161798144} - \frac{14424400165163864701 \log(7)}{25480396800} \right) e^{12} \\ + \left(-\frac{4506759544919422111 \log(2)}{444528000} + \frac{4528120073662511265537 \log(3)}{1438646272000} - \frac{12939671783145268046875 \log(5)}{22373826822144} + \frac{17394718021348645585769 \log(7)}{8153726976000} \right. \\ \left. + \frac{81402749386839761113321 \log(11)}{559345670553600} \right) e^{14} + \left(\frac{8175474265144902875339 \log(2)}{192036096000} - \frac{487753344707796027586053 \log(3)}{23018340352000} + \frac{8271291205691128966015625 \log(5)}{1073943687462912} \right. \\ \left. - \frac{6796075855660208932297721 \log(7)}{1174136684544000} - \frac{1236467363350808533619347277 \log(11)}{402728882798592000} \right) e^{16} + \dots, \quad (4.9)$$

$$\Delta\psi_{5L}^p = \left(\frac{11153}{35} + \frac{11341e^2}{15} + \frac{46467e^4}{280} - \frac{1119e^6}{560} \right). \quad (4.10)$$

Like the redshift invariant, the first half-integer function appears at 5.5PN order. We find it to be a rational-number infinite series, multiplied by an overall factor of π

$$\Delta\psi_{11/2}^p = \pi \left(\frac{49969}{315} + \frac{319609e^2}{630} + \frac{21280909e^4}{100800} + \frac{2619467e^6}{362880} - \frac{5582939e^8}{580608000} + \frac{19566341e^{10}}{5806080000} \right. \\ \left. - \frac{1283076269e^{12}}{2601123840000} - \frac{3498178499e^{14}}{21849440256000} + \frac{4868320009201e^{16}}{251705551749120000} + \dots \right). \quad (4.11)$$

At 6PN order we found a structure similar to 4PN and 5PN, but with some added complexity. Once again, we were able to find a closed-form expression for the (6PN) log term, though it is not simply a polynomial. The 6PN log

term reappears in the 6PN non-log function. We group the log-transcendental number terms into a χ -like series again. Then, an added wrinkle is the appearance of a π^4 term (which is a polynomial in e) as well as a more complicated closed-form expression multiplying π^2 . The remainder is, again, a rational-number series. This breakdown is given by

$$\begin{aligned} \Delta\psi_6^p = & \left(-\frac{1900873914203}{101606400} - \frac{465224579689e^2}{5080320} - \frac{2021344615177e^4}{33868800} - \frac{481812394033e^6}{203212800} \right. \\ & + \frac{908657975293e^8}{1625702400} + \frac{115787009753e^{10}}{464486400} + \frac{63855468847e^{12}}{371589120} + \frac{663864852377e^{14}}{5202247680} \\ & + \frac{237445545371e^{16}}{2378170368} + \dots \Big) + \pi^4 \left(-\frac{7335303}{131072} - \frac{146026515e^2}{1048576} - \frac{17998485e^4}{524288} + \frac{679545e^6}{16777216} \right) \\ & + \pi^2 \left[\frac{7254777827}{2359296} + \frac{32034966215e^2}{2359296} + \frac{77315025809e^4}{9437184} + \frac{5875228633e^6}{12582912} - \frac{326041715e^8}{33554432} \right. \\ & + \left(-\frac{21405}{2048} - \frac{26549e^2}{8192} \right) (1-e^2)^{5/2} \Big] - 2 \left[\gamma_E + \log \left(\frac{8(1-e^2)^{3/2}}{1+\sqrt{1-e^2}} \right) \right] \Delta\psi_{6L}^p + \Delta\psi_6^{p,\chi}, \end{aligned} \quad (4.12)$$

$$\begin{aligned} \Delta\psi_6^{p,\chi} = & \left[\left(-\frac{5637649 \log(2)}{630} + \frac{234009 \log(3)}{70} + \frac{9765625 \log(5)}{9072} \right) + \left(\frac{278347639 \log(2)}{945} - \frac{159335343 \log(3)}{8960} \right. \right. \\ & - \frac{17193359375 \log(5)}{145152} \Big) e^2 + \left(-\frac{67298137969 \log(2)}{15120} - \frac{6160676211 \log(3)}{4480} + \frac{2073211184375 \log(5)}{870912} \right. \\ & + \frac{96889010407 \log(7)}{248832} \Big) e^4 + \left(\frac{45349640544529 \log(2)}{816480} + \frac{31165257813381 \log(3)}{1146880} \right. \\ & - \frac{182206079940625 \log(5)}{7962624} - \frac{387081765684929 \log(7)}{23887872} \Big) e^6 + \left(-\frac{558659555193209 \log(2)}{816480} \right. \\ & - \frac{53870960843541 \log(3)}{262144} + \frac{61171359261321875 \log(5)}{445906944} + \frac{294158696797354949 \log(7)}{1194393600} \Big) e^8 \\ & + \left(\frac{847397764060731841 \log(2)}{122472000} + \frac{32809717319486013 \log(3)}{1835008000} - \frac{2422221742760078125 \log(5)}{5350883328} \right. \\ & - \frac{2408276754022760847373 \log(7)}{1146617856000} \Big) e^{10} + \left(-\frac{16872974428064804681 \log(2)}{321489000} \right. \\ & + \frac{702548354497142812293 \log(3)}{51380224000} - \frac{10596237215626599434375 \log(5)}{5393690394624} \\ & + \frac{16313635952096120303239 \log(7)}{1375941427200} + \frac{81402749386839761113321 \log(11)}{134842259865600} \Big) e^{12} \\ & + \left(\frac{44527790291197983392407 \log(2)}{144027072000} - \frac{796933093810646955107709 \log(3)}{5754585088000} \right. \\ & + \frac{110679665407920978635528125 \log(5)}{2416373296791552} - \frac{42403949775722831599753919 \log(7)}{880602513408000} \\ & - \frac{151763386707026658481899113 \log(11)}{8629904631398400} \Big) e^{14} + \left(-\frac{1066795518870736337912533 \log(2)}{691329945600} \right. \\ & + \frac{561883567881441059477453079 \log(3)}{736586891264000} - \frac{68528286383578337812136246875 \log(5)}{173978877368991744} \\ & + \frac{18715907817618872220720781253 \log(7)}{126806761930752000} + \frac{624926196399309721148911875383 \log(11)}{2718419958890496000} \\ & + \frac{91733330193268616658399616009 \log(13)}{8698943868449587200} \Big) e^{16} + \dots \Big], \end{aligned} \quad (4.13)$$

$$\Delta\psi_{6L}^p = \frac{454397}{3780} + \frac{2384929e^2}{1890} + \frac{45143023e^4}{30240} + \frac{5037481e^6}{20160} - \frac{2387e^8}{960} - \left(\frac{146}{5} + \frac{37e^2}{5} \right) (1-e^2)^{5/2}. \quad (4.14)$$

The 6.5PN term is similar in form to the 5.5PN term, a rational-number infinite series with an overall factor of π

$$\Delta\psi_{13/2}^p = \pi \left(-\frac{2620819}{2100} - \frac{1586616631e^2}{235200} - \frac{5337465431e^4}{940800} - \frac{273779628487e^6}{406425600} \right.$$

$$\begin{aligned}
& + \frac{23921441479e^8}{5419008000} - \frac{2200323829e^{10}}{19267584000} + \frac{6113757813097e^{12}}{655483207680000} \\
& + \frac{200661326003101e^{14}}{48942746173440000} - \frac{13890607636693243e^{16}}{7047755448975360000} + \dots \Big). \tag{4.15}
\end{aligned}$$

At 7PN order, there are additional complexities. Here, a $\log^2 p$ term makes its first appearance and we find the closed-form expression for that term. The 7PN log term then inherits the general structure of the 4PN non-log term. It features a reappearance of the 7PN $\log^2 p$ term, a χ -like series grouping, and a remaining rational-number series. The 7PN non-log term is the first appearance of a much more complicated expansion, which features numerous transcendental number terms. While we have calculated it to e^{16} , it is sufficiently complicated that we only present the first few coefficients here. The entire term is available online [50, 51]. The breakdown of the 7PN terms is

$$\begin{aligned}
\Delta\psi_7^p = & \left(-\frac{1282190594044678657}{7041323520000} + \frac{1316474014843\gamma_E}{43659000} - \frac{3396608\gamma_E^2}{1575} + \frac{25657561505749\pi^2}{2477260800} \right. \\
& + \frac{341587582057\pi^4}{1006632960} + \frac{2783260080883 \log(2)}{43659000} - \frac{5149696\gamma_E \log(2)}{1575} - \frac{931328 \log^2(2)}{1575} \\
& + \frac{282123979047 \log(3)}{8624000} - \frac{936036}{175} \gamma_E \log(3) - \frac{936036}{175} \log(2) \log(3) - \frac{468018 \log^2(3)}{175} + \frac{63488\zeta(3)}{15} \\
& \left. - \frac{361328125 \log(5)}{24192} \right) + \left(-\frac{2888955324477314921}{2347107840000} + \frac{1075057978433\gamma_E}{4851000} - \frac{7219504\gamma_E^2}{525} \right. \\
& + \frac{465082867177871\pi^2}{6606028800} + \frac{314165501411\pi^4}{335544320} + \frac{2387982140729 \log(2)}{8731800} - \frac{79652512}{315} \gamma_E \log(2) \\
& - \frac{80263696 \log^2(2)}{175} - \frac{299782486660473 \log(3)}{275968000} + \frac{15912612}{175} \gamma_E \log(3) + \frac{15912612}{175} \log(2) \log(3) \\
& + \frac{7956306 \log^2(3)}{175} + \frac{2411543359375 \log(5)}{2838528} + \frac{678223072849 \log(7)}{6082560} + \frac{134944\zeta(3)}{5} \Big) e^2 \\
& + \left(-\frac{113070994466917771}{58677696000} + \frac{1472132397523\gamma_E}{4656960} - \frac{1627684\gamma_E^2}{105} + \frac{1927756649323\pi^2}{18350080} \right. \\
& - \frac{230109551791\pi^4}{268435456} + \frac{4388818385774297 \log(2)}{349272000} + \frac{1697626904}{525} \gamma_E \log(2) + \frac{3404199436 \log^2(2)}{525} \\
& + \frac{157855832267967 \log(3)}{7168000} - \frac{262324089}{400} \gamma_E \log(3) - \frac{262324089}{400} \log(2) \log(3) - \frac{262324089 \log^2(3)}{800} \\
& - \frac{7905614284523125 \log(5)}{1072963584} - \frac{1044921875\gamma_E \log(5)}{1008} - \frac{1044921875 \log(2) \log(5)}{1008} \\
& \left. - \frac{1044921875 \log^2(5)}{2016} - \frac{1107664826873969 \log(7)}{109486080} + 30424\zeta(3) \right) e^4 + \dots, \tag{4.16}
\end{aligned}$$

$$\begin{aligned}
\Delta\psi_{7L}^p = & \left(-\frac{1316474014843}{87318000} - \frac{1048904096833e^2}{9702000} - \frac{6494255602463e^4}{46569600} - \frac{2123271392639e^6}{55883520} \right. \\
& - \frac{1333068673e^8}{352800} - \frac{148643207731e^{10}}{88704000} - \frac{5888596871e^{12}}{5376000} - \frac{204908923e^{14}}{258048} \\
& \left. - \frac{63078518299e^{16}}{103219200} + \dots \right) - 4 \left[\gamma_E + \log \left(\frac{8(1-e^2)^{3/2}}{1+\sqrt{1-e^2}} \right) \right] \Delta\psi_{7L2}^p + \Delta\psi_{7L}^{p,\chi}, \tag{4.17}
\end{aligned}$$

$$\begin{aligned}
\Delta\psi_{7L}^{p,\chi} = & \left(-\frac{602624 \log(2)}{225} + \frac{468018 \log(3)}{175} \right) + \left(\frac{155814256 \log(2)}{1575} - \frac{7956306 \log(3)}{175} \right) e^2 \\
& + \left(-\frac{865090292 \log(2)}{525} + \frac{262324089 \log(3)}{800} + \frac{1044921875 \log(5)}{2016} \right) e^4 + \left(\frac{7561620022 \log(2)}{525} \right. \\
& + \frac{418174083 \log(3)}{200} - \frac{11494140625 \log(5)}{1512} \Big) e^6 + \left(-\frac{27112112493049 \log(2)}{283500} \right. \\
& \left. - \frac{339134405423319 \log(3)}{7168000} + \frac{238205615234375 \log(5)}{4644864} + \frac{507989081563901 \log(7)}{27648000} \right) e^8
\end{aligned}$$

$$\begin{aligned}
& + \left(\frac{2438441188502 \log(2)}{3375} + \frac{2457755729168913 \log(3)}{7168000} - \frac{328215185546875 \log(5)}{1548288} - \right. \\
& \left. \frac{507989081563901 \log(7)}{1843200} \right) e^{10} + \left(- \frac{27531157668664681 \log(2)}{4961250} - \frac{6481474893571248729 \log(3)}{8028160000} \right. \\
& \left. + \frac{2822922907568359375 \log(5)}{4682022912} + \frac{92389498231271366573 \log(7)}{47775744000} \right) e^{12} + \\
& \left(\frac{20936989659899360021 \log(2)}{625117500} - \frac{171956257323847250841 \log(3)}{28098560000} - \frac{510786718173828125 \log(5)}{16387080192} \right. \\
& \left. - \frac{1009210224594126146977 \log(7)}{119439360000} \right) e^{14} + \left(- \frac{4619194353324708185237 \log(2)}{30005640000} \right. \\
& + \frac{982128291923792960826417 \log(3)}{14386462720000} - \frac{2383328610155127138671875 \log(5)}{134242960932864} \\
& \left. + \frac{18946304992805061334986887 \log(7)}{733835427840000} + \frac{1053921396311414387134166987 \log(11)}{251705551749120000} \right) e^{16} + \dots,
\end{aligned} \tag{4.18}$$

$$\Delta\psi_{7L2}^p = -\frac{849152}{1575} - \frac{1804876e^2}{525} - \frac{406921e^4}{105} - \frac{543667e^6}{630} - \frac{10593e^8}{560}. \tag{4.19}$$

The 7.5PN term is a rational-number infinite series (multiplied by an overall factor of π), like the two half-integer contributions before it

$$\begin{aligned}
\Delta\psi_{15/2}^p = \pi & \left(\frac{2782895449}{2910600} + \frac{2404331748779e^2}{279417600} + \frac{76598649855971e^4}{6035420160} + \frac{8047650291899e^6}{5267275776} \right. \\
& - \frac{5292862534207931e^8}{10534551552000} - \frac{279109475326162289e^{10}}{27811216097280000} - \frac{4713058120092455293e^{12}}{2336142152171520000} \\
& \left. - \frac{959696950970026746929e^{14}}{523295842086420480000} - \frac{25409776245923969873e^{16}}{37378274434744320000} + \dots \right).
\end{aligned} \tag{4.20}$$

The description of the breakdown in the 8PN eccentricity functions is essentially the same as what we said about the 7PN terms just prior to (4.16). We still find a polynomial for the 8PN $\log^2 p$ term, albeit one order in e^2 longer. Because of the complexity of the 8PN non-log term, we give it only through e^4 and leave the full expansion through e^{16} to the online repositories [50, 51]. The 8PN spin-precession-invariant correction splits into

$$\begin{aligned}
\Delta\psi_8^p = & \left(\frac{78550205239878250993769}{28193459374080000} - \frac{1888832198890393\gamma_E}{15891876000} + \frac{177306208\gamma_E^2}{11025} + \frac{569460279231731\pi^2}{123312537600} \right. \\
& - \frac{623848083842333\pi^4}{21474836480} - \frac{41942063811247 \log(2)}{1059458400} + \frac{2720192\gamma_E \log(2)}{11025} - \frac{520925728 \log^2(2)}{11025} \\
& - \frac{868469344973829 \log(3)}{3139136000} + \frac{59742279\gamma_E \log(3)}{1225} + \frac{59742279 \log(2) \log(3)}{1225} + \frac{59742279 \log^2(3)}{2450} \\
& + \frac{8570767578125 \log(5)}{96864768} + \frac{678223072849 \log(7)}{92664000} - \frac{861696\zeta(3)}{35} \left. \right) + \left(\frac{12590844685671737819611}{939781979136000} \right. \\
& - \frac{3978068608616891\gamma_E}{2648646000} + \frac{371280152\gamma_E^2}{2205} - \frac{33310259864964463\pi^2}{443925135360} - \frac{31118085613898053\pi^4}{257698037760} \\
& - \frac{88630614687481099 \log(2)}{7945938000} + \frac{38342498672\gamma_E \log(2)}{11025} + \frac{7893208952 \log^2(2)}{1225} + \frac{812331139710343959 \log(3)}{100452352000} \\
& - \frac{621149553}{784} \gamma_E \log(3) - \frac{621149553}{784} \log(2) \log(3) - \frac{621149553 \log^2(3)}{1568} - \frac{196313675703125 \log(5)}{21697708032} \\
& - \frac{3173828125\gamma_E \log(5)}{7056} - \frac{3173828125 \log(2) \log(5)}{7056} - \frac{3173828125 \log^2(5)}{14112} - \frac{55100101995388051 \log(7)}{23721984000} \\
& \left. - \frac{5551264\zeta(3)}{21} \right) e^2 + \left(\frac{3657307066227250447201}{293681868480000} - \frac{159538901113146521\gamma_E}{42378336000} + \frac{397837653\gamma_E^2}{1225} \right. \\
& - \frac{384067364086852189\pi^2}{2959500902400} - \frac{4915898447923097\pi^4}{85899345920} + \frac{82885306824453137 \log(2)}{54486432000} \\
& \left. - \frac{246163497086\gamma_E \log(2)}{4725} - \frac{482425731551 \log^2(2)}{4725} - \frac{16338364486486698339 \log(3)}{200904704000} + \frac{15151367601\gamma_E \log(3)}{78400} \right)
\end{aligned}$$

$$\begin{aligned}
& -\frac{456484805199 \log(2) \log(3)}{78400} + \frac{15151367601 \log^2(3)}{156800} - \frac{12490894332540370625 \log(5)}{130186248192} \\
& + \frac{2022790234375 \gamma_E \log(5)}{84672} + \frac{2022790234375 \log(2) \log(5)}{84672} + \frac{2022790234375 \log^2(5)}{169344} \\
& + \frac{16777483050927098843 \log(7)}{142331904000} - \frac{17811754 \zeta(3)}{35} \Big) e^4 + \dots, \tag{4.21}
\end{aligned}$$

$$\begin{aligned}
\Delta\psi_{8L}^p = & \left(\frac{1884153630595993}{31783752000} + \frac{3866001511074491e^2}{5297292000} + \frac{140691202491074201e^4}{84756672000} + \frac{8446543158422249e^6}{9246182400} \right. \\
& + \frac{2393628746500801e^8}{16951334400} + \frac{8815849170404069e^{10}}{226017792000} + \frac{37201967185037e^{12}}{1549836288} + \frac{5703127370959e^{14}}{338688000} \\
& \left. + \frac{6115396987321e^{16}}{481689600} + \dots \right) - 4 \left[\gamma_E + \log \left(\frac{8(1-e^2)^{3/2}}{1+\sqrt{1-e^2}} \right) \right] \Delta\psi_{8L2}^p + \Delta\psi_{8L}^{p,x}, \tag{4.22}
\end{aligned}$$

$$\begin{aligned}
\Delta\psi_{8L}^{p,x} = & \left(\frac{70650464 \log(2)}{2205} - \frac{59742279 \log(3)}{2450} \right) + \left(-\frac{2208349688 \log(2)}{1575} + \frac{621149553 \log(3)}{1568} \right. \\
& + \frac{3173828125 \log(5)}{14112} \Big) e^2 + \left(\frac{883055473063 \log(2)}{33075} - \frac{15151367601 \log(3)}{156800} - \frac{2022790234375 \log(5)}{169344} \right) e^4 \\
& + \left(-\frac{9735335606114 \log(2)}{33075} - \frac{2983923884637 \log(3)}{28672} + \frac{2682838643359375 \log(5)}{16257024} \right. \\
& + \frac{8816899947037 \log(7)}{331776} \Big) e^6 + \left(\frac{23310192268124059 \log(2)}{7938000} + \frac{302771958934455009 \log(3)}{200704000} \right. \\
& \left. - \frac{156689829056640625 \log(5)}{130056192} - \frac{299112464634116791 \log(7)}{331776000} \right) e^8 + \dots, \tag{4.23}
\end{aligned}$$

$$\Delta\psi_{8L2}^p = \frac{44326552}{11025} + \frac{92820038e^2}{2205} + \frac{397837653e^4}{4900} + \frac{155002853e^6}{4410} + \frac{332684587e^8}{141120} - \frac{100899e^{10}}{6272}. \tag{4.24}$$

B. Spin-precession invariant as an expansion in y

The compactness parameter $1/p$ is easily related to e and the alternative compactness parameter y , written as a PN expansion. That relationship allows (4.1) to be recast as an expansion in y

$$\begin{aligned}
\Delta\psi = & \Delta\psi_1^y y + \Delta\psi_2^y y^2 + \Delta\psi_3^y y^3 + (\Delta\psi_4^y + \Delta\psi_{4L}^y \log y) y^4 + (\Delta\psi_5^y + \Delta\psi_{5L}^y \log y) y^5 + \Delta\psi_{11/2}^y y^{11/2} \\
& + (\Delta\psi_6^y + \Delta\psi_{6L}^y \log y) y^6 + \Delta\psi_{13/2}^y y^{13/2} + (\Delta\psi_7^y + \Delta\psi_{7L}^y \log y + \Delta\psi_{7L2}^y \log^2 y) y^7 + \Delta\psi_{15/2}^y y^{15/2} \\
& + (\Delta\psi_8^y + \Delta\psi_{8L}^y \log y + \Delta\psi_{8L2}^y \log^2 y) y^8 + (\Delta\psi_{17/2}^y + \Delta\psi_{17/2}^y \log y) y^{17/2} \\
& + (\Delta\psi_9^y + \Delta\psi_{9L}^y \log y + \Delta\psi_{9L2}^y \log^2 y) y^9 + \dots. \tag{4.25}
\end{aligned}$$

Again, the entire right hand side should be viewed as multiplied by a factor of μ/M . Because of the reparameterization, many of the functions $\Delta\psi_k^y(e)$ differ from their analogs $\Delta\psi_k^p(e)$ in the prior subsection.

The first three terms differ from (4.2)-(4.4) but still have simple closed forms

$$\Delta\psi_1^y = \frac{-1}{1-e^2}, \tag{4.26}$$

$$\Delta\psi_2^y = \frac{1}{(1-e^2)^2} \left(\frac{9}{4} + 3e^2 \right), \tag{4.27}$$

$$\Delta\psi_3^y = \frac{1}{(1-e^2)^3} \left(\frac{819}{16} - \frac{123\pi^2}{64} + e^2 \left(\frac{173}{16} - \frac{123\pi^2}{256} \right) - \frac{15e^4}{2} \right) - \frac{5}{(1-e^2)^{3/2}}. \tag{4.28}$$

Note the appearance of eccentricity singular factors of increasing power.

The rest of the terms closely mirror their counterparts in the $1/p$ expansion. We will refer the reader back to the previous subsection for discussion. The 4PN terms are similar in form to those in (4.5), (4.6), and (4.7)

$$\Delta\psi_4^y = \frac{1}{(1-e^2)^4} \left(-\frac{587831}{2880} - \frac{82781e^2}{160} - \frac{99259e^4}{480} + \frac{15821e^6}{1152} - \frac{100147e^8}{15360} - \frac{10451e^{10}}{2048} \right)$$

$$\begin{aligned}
& -\frac{291445e^{12}}{73728} - \frac{51573e^{14}}{16384} - \frac{674917e^{16}}{262144} + \dots \Big) + \frac{\pi^2}{(1-e^2)^4} \left(\frac{31697}{6144} + \frac{23503e^2}{4096} + \frac{23471e^4}{16384} \right) \\
& + 2 \left[\gamma_E + \log \left(\frac{8(1-e^2)}{1+\sqrt{1-e^2}} \right) \right] \Delta\psi_{4L}^y + \Delta\psi_4^{y,x}, \tag{4.29} \\
\Delta\psi_4^{y,x} = & \frac{1}{(1-e^2)^4} \left[\left(\frac{729\log(3)}{5} - \frac{2216\log(2)}{15} \right) + \left(\frac{55384\log(2)}{15} - \frac{10206\log(3)}{5} \right) e^2 + \left(\frac{3620943\log(3)}{320} - \right. \right. \\
& \frac{205917\log(2)}{5} + \frac{1953125\log(5)}{192} \Big) e^4 + \left(\frac{11518508\log(2)}{45} + \frac{3995649\log(3)}{320} - \frac{68359375\log(5)}{576} \right) e^6 \\
& + \left(\frac{274244140625\log(5)}{442368} - \frac{1597223897\log(2)}{1350} - \frac{199689627159\log(3)}{409600} + \frac{678223072849\log(7)}{3686400} \right) e^8 \\
& + \left(\frac{27567693977\log(2)}{4500} + \frac{1474172887599\log(3)}{512000} - \frac{71310546875\log(5)}{36864} - \frac{678223072849\log(7)}{307200} \right) \\
& \times e^{10} + \left(-\frac{39584616236117\log(2)}{1134000} - \frac{2523359744732097\log(3)}{458752000} + \frac{1806540009765625\log(5)}{445906944} \right. \\
& + \frac{77643655602826369\log(7)}{6370099200} \Big) e^{12} + \left(\frac{7796904819020377\log(2)}{47628000} - \frac{96876093468033783\log(3)}{3211264000} - \right. \\
& \frac{173056322265625\log(5)}{3121348608} - \frac{1313351173426101691\log(7)}{31850496000} \Big) e^{14} + \left(-\frac{1349495913968063023\log(2)}{2286144000} \right. \\
& + \frac{44537688184006902231\log(3)}{164416716800} - \frac{131695624109951171875\log(5)}{1826434842624} \\
& + \frac{9397785802951526436547\log(7)}{97844723712000} + \frac{81402749386839761113321\log(11)}{4794391461888000} \Big) e^{16} + \dots \Big], \tag{4.30} \\
\Delta\psi_{4L}^y = & \frac{1}{(1-e^2)^4} \left(\frac{628}{15} + \frac{268e^2}{5} + \frac{37e^4}{10} \right). \tag{4.31}
\end{aligned}$$

The polynomial part of the 4PN log term is identical to that in (4.7), reflecting its nature as a leading-logarithm term. Like the 4PN term in the $1/p$ expansion, we also calculated this term in the y expansion to e^{30} , and that entire dependence is reproduced in the online repositories [50, 51].

The 5PN terms mirror those in (4.8), (4.9), and (4.10)

$$\begin{aligned}
\Delta\psi_5^y = & \frac{1}{(1-e^2)^5} \left(-\frac{48221551}{19200} - \frac{218002469e^2}{134400} + \frac{554849699e^4}{134400} + \frac{15403763e^6}{9600} + \frac{45454391e^8}{215040} \right. \\
& + \frac{175906613e^{10}}{1075200} + \frac{9382421e^{12}}{81920} + \frac{147111571e^{14}}{1720320} + \frac{736852183e^{16}}{11010048} + \dots \Big) \\
& + \frac{\pi^2}{(1-e^2)^5} \left[\frac{2719317}{8192} + \frac{6391663e^2}{16384} - \frac{1142291e^4}{65536} - \frac{223697e^6}{65536} - (1-e^2)^{3/2} \left(\frac{7503}{256} + \frac{861e^2}{128} \right) \right] \\
& + 2 \left[\gamma_E + \log \left(\frac{8(1-e^2)}{1+\sqrt{1-e^2}} \right) \right] \Delta\psi_{5L}^y + \Delta\psi_5^{y,x}, \tag{4.32} \\
\Delta\psi_5^{y,x} = & \frac{1}{(1-e^2)^5} \left[\left(\frac{155894\log(2)}{105} - \frac{31347\log(3)}{28} \right) + \left(-\frac{292974\log(2)}{7} + \frac{811377\log(3)}{64} \right. \right. \\
& + \frac{9765625\log(5)}{1344} \Big) e^2 + \left(\frac{98443429\log(2)}{180} - \frac{11825109\log(3)}{8960} - \frac{3850703125\log(5)}{16128} \right) e^4 + \\
& \left(\frac{179751484375\log(5)}{73728} - \frac{33799060013\log(2)}{7560} - \frac{438821183313\log(3)}{286720} + \frac{96889010407\log(7)}{221184} \right) e^6 \\
& + \left(\frac{1285645374023\log(2)}{37800} + \frac{192170674772001\log(3)}{11468800} - \frac{167918368984375\log(5)}{12386304} \right. \\
& - \frac{458460436354739\log(7)}{44236800} \Big) e^8 + \left(-\frac{62011700285317\log(2)}{226800} - \frac{6866280939571821\log(3)}{91750400} + \right. \\
& \frac{7306249357578125\log(5)}{148635648} + \frac{350314344636373817\log(7)}{3538944000} \Big) e^{10} + \left(\frac{178662406711739429\log(2)}{95256000} - \right.
\end{aligned}$$

$$\begin{aligned}
& \frac{1101374969180716197 \log(3)}{12845056000} - \frac{358568725832265625 \log(5)}{4161798144} - \frac{13974363888728765053 \log(7)}{25480396800} \Big) e^{12} \\
& + \left(-\frac{4382622188402959199 \log(2)}{444528000} + \frac{4591426122938350115073 \log(3)}{1438646272000} \right. \\
& - \frac{4554943798461756015625 \log(5)}{7457942274048} + \frac{16599646987975703567209 \log(7)}{8153726976000} \\
& + \frac{81402749386839761113321 \log(11)}{559345670553600} \Big) e^{14} + \left(\frac{7923977303302581594827 \log(2)}{192036096000} \right. \\
& - \frac{482198082003965098333701 \log(3)}{23018340352000} + \frac{8271767545294840966015625 \log(5)}{1073943687462912} \\
& - \frac{6408752834402770430401529 \log(7)}{1174136684544000} - \frac{1236467363350808533619347277 \log(11)}{402728882798592000} \Big) e^{16} + \dots \Big], \tag{4.33}
\end{aligned}$$

$$\Delta\psi_{5L}^y = -\frac{1}{(1-e^2)^5} \left(\frac{11153}{35} + 1091e^2 + \frac{166531e^4}{280} + \frac{15457e^6}{560} \right). \tag{4.34}$$

The polynomial part of the 5PN log term differs from that in (4.10), as expected since it is a 1PN-log (i.e., a 1PN correction to a leading log) [4].

The 5.5PN (first half-integer PN) term is similar to its $1/p$ expansion (4.11)

$$\begin{aligned}
\Delta\psi_{11/2}^y = & \frac{\pi}{(1-e^2)^{11/2}} \left(\frac{49969}{315} + \frac{319609e^2}{630} + \frac{21280909e^4}{100800} + \frac{2619467e^6}{362880} - \frac{5582939e^8}{580608000} \right. \\
& + \frac{19566341e^{10}}{5806080000} - \frac{1283076269e^{12}}{2601123840000} - \frac{3498178499e^{14}}{21849440256000} + \frac{4868320009201e^{16}}{251705551749120000} + \dots \Big). \tag{4.35}
\end{aligned}$$

The 6PN term splits into parts that mimic (4.12), (4.13), and (4.14) in the $1/p$ expansion of the 6PN term, with the exception of the appearance of eccentricity singular factors

$$\begin{aligned}
\Delta\psi_6^y = & \frac{1}{(1-e^2)^6} \left(-\frac{1900873914203}{101606400} - \frac{327006360319e^2}{5080320} - \frac{1043250935257e^4}{33868800} - \frac{5158311322393e^6}{203212800} \right. \\
& - \frac{14506405082507e^8}{1625702400} - \frac{869231282527e^{10}}{464486400} - \frac{86093410741e^{12}}{74317824} - \frac{4056226220383e^{14}}{5202247680} - \frac{1350712174045e^{16}}{2378170368} \Big) \\
& + \frac{\pi^4}{(1-e^2)^6} \left(-\frac{7335303}{131072} - \frac{146026515e^2}{1048576} - \frac{17998485e^4}{524288} + \frac{679545e^6}{16777216} \right) + \frac{\pi^2}{(1-e^2)^6} \left[\left(\frac{215485}{6144} \right. \right. \\
& + \frac{1156631e^2}{8192} + \frac{280939e^4}{8192} \Big) (1-e^2)^{3/2} + \frac{7147373027}{2359296} + \frac{24774167687e^2}{2359296} + \frac{38112094481e^4}{9437184} \\
& + \frac{7266864217e^6}{12582912} + \frac{445428621e^8}{33554432} \Big] + 2 \left[\gamma_E + \log \left(\frac{8(1-e^2)}{1+\sqrt{1-e^2}} \right) \right] \Delta\psi_{6L}^y + \Delta\psi_6^{y,x} \\
\Delta\psi_6^{y,x} = & \frac{1}{(1-e^2)^6} \left[\left(-\frac{5637649 \log(2)}{630} + \frac{234009 \log(3)}{70} + \frac{9765625 \log(5)}{9072} \right) + \left(\frac{38238253 \log(2)}{135} \right. \right. \\
& - \frac{18075555 \log(3)}{1792} - \frac{17193359375 \log(5)}{145152} \Big) e^2 + \left(-\frac{12445643645 \log(2)}{3024} - \frac{6533011503 \log(3)}{4480} \right. \\
& + \frac{2009929934375 \log(5)}{870912} + \frac{96889010407 \log(7)}{248832} \Big) e^4 + \left(\frac{8316214161581 \log(2)}{163296} + \frac{30954590856837 \log(3)}{1146880} \right. \\
& - \frac{1155970259584375 \log(5)}{55738368} - \frac{387081765684929 \log(7)}{23887872} \Big) e^6 + \left(-\frac{525941334093929 \log(2)}{816480} \right. \\
& - \frac{1751622570112671 \log(3)}{9175040} + \frac{51404505486321875 \log(5)}{445906944} + \frac{288926690235376949 \log(7)}{1194393600} \Big) e^8 \\
& + \left(\frac{808070130394854601 \log(2)}{122472000} - \frac{254004783448418307 \log(3)}{1835008000} - \frac{1753181559747578125 \log(5)}{5350883328} \right. \\
& - \frac{2294506717029507369613 \log(7)}{1146617856000} \Big) e^{10} + \left(-\frac{16027246190731123427 \log(2)}{321489000} \right.
\end{aligned}$$

$$\begin{aligned}
& + \frac{738364400868241156581 \log(3)}{51380224000} - \frac{13119943727175549434375 \log(5)}{5393690394624} \\
& + \frac{15015279849631826906071 \log(7)}{1375941427200} + \frac{81402749386839761113321 \log(11)}{134842259865600} \Big) e^{12} \\
& + \left(\frac{41914674050681714318023 \log(2)}{144027072000} - \frac{791847483991723599711741 \log(3)}{5754585088000} \right. \\
& + \frac{112698947723278715435528125 \log(5)}{2416373296791552} - \frac{37760848394198321304112319 \log(7)}{880602513408000} \\
& \left. - \frac{151763386707026658481899113 \log(11)}{8629904631398400} \right) e^{14} + \left(- \frac{5002336841855648660824877 \log(2)}{3456649728000} \right. \\
& + \frac{539059140139095745481254167 \log(3)}{736586891264000} - \frac{67491579530903875816811246875 \log(5)}{173978877368991744} \\
& + \frac{16203069304365251842129022021 \log(7)}{126806761930752000} + \frac{620970022779109308758804474783 \log(11)}{2718419958890496000} \\
& \left. + \frac{91733330193268616658399616009 \log(13)}{8698943868449587200} \right) e^{16} + \dots \Big], \tag{4.36}
\end{aligned}$$

$$\begin{aligned}
\Delta\psi_{6L}^y &= \frac{1}{(1-e^2)^6} \left(-\frac{3619517}{3780} + \frac{2086379e^2}{1890} + \frac{236556689e^4}{30240} + \frac{67767047e^6}{20160} + \frac{777533e^8}{6720} \right) \\
&+ \frac{1}{(1-e^2)^{9/2}} \left(\frac{12998}{15} + \frac{5251e^2}{5} + \frac{333e^4}{5} \right). \tag{4.37}
\end{aligned}$$

The 6.5PN term is a rational-number infinite series similar to that in the 5.5PN term and the $1/p$ expansion 6.5PN term (4.15), except for a higher power eccentricity singular factor

$$\begin{aligned}
\Delta\psi_{13/2}^y &= \frac{\pi}{(1-e^2)^{13/2}} \left(-\frac{2620819}{2100} - \frac{5991086053e^2}{705600} - \frac{31762727813e^4}{2822400} - \frac{243526100891e^6}{81285120} \right. \\
&- \frac{1219109013163e^8}{16257024000} - \frac{4383296599e^{10}}{520224768000} - \frac{18184820155799e^{12}}{655483207680000} \\
&\left. + \frac{93245463971129e^{14}}{9788549234688000} - \frac{1478510613681403e^{16}}{7047755448975360000} + \dots \right). \tag{4.38}
\end{aligned}$$

The 7PN term reflects the split seen in (4.16), (4.17), (4.18), and with a new 7PN $\log^2 y$ term like (4.19)

$$\begin{aligned}
\Delta\psi_7^y &= \frac{1}{(1-e^2)^7} \left[-\frac{1282190594044678657}{7041323520000} + \frac{1316474014843\gamma_E}{43659000} - \frac{3396608\gamma_E^2}{1575} + \frac{25657561505749\pi^2}{2477260800} \right. \\
&+ \frac{341587582057\pi^4}{1006632960} + \frac{2783260080883 \log(2)}{43659000} - \frac{5149696\gamma_E \log(2)}{1575} - \frac{931328 \log^2(2)}{1575} + \frac{63488\zeta(3)}{15} \\
&+ \frac{282123979047 \log(3)}{8624000} - \frac{936036}{175} \gamma_E \log(3) - \frac{936036}{175} \log(2) \log(3) - \frac{468018 \log^2(3)}{175} \\
&- \frac{361328125 \log(5)}{24192} + \left(-\frac{2138140154533483481}{2347107840000} + \frac{1128946342193\gamma_E}{4851000} - \frac{7219504\gamma_E^2}{525} \right. \\
&+ \frac{163472352568271\pi^2}{6606028800} + \frac{539506009571\pi^4}{335544320} + \frac{3277934193257 \log(2)}{8731800} - \frac{79652512}{315} \gamma_E \log(2) \\
&- \frac{80263696 \log^2(2)}{175} - \frac{306185205247353 \log(3)}{275968000} + \frac{15912612}{175} \gamma_E \log(3) + \frac{15912612}{175} \log(2) \log(3) \\
&+ \frac{7956306 \log^2(3)}{175} + \frac{1017804296875 \log(5)}{1216512} + \frac{678223072849 \log(7)}{6082560} + \frac{134944\zeta(3)}{5} \Big) e^2 \\
&+ \left(-\frac{188303307112006921}{234710784000} + \frac{8205409254671\gamma_E}{23284800} - \frac{1627684\gamma_E^2}{105} - \frac{2849889305071\pi^2}{55050240} \right. \\
&+ \frac{218483902289\pi^4}{268435456} + \frac{3490527652132457 \log(2)}{349272000} + \frac{1697626904}{525} \gamma_E \log(2) + \frac{3404199436 \log^2(2)}{525} \\
&\left. + \frac{157927289197887 \log(3)}{7168000} - \frac{262324089}{400} \gamma_E \log(3) - \frac{262324089}{400} \log(2) \log(3) - \frac{262324089 \log^2(3)}{800} \right)
\end{aligned}$$

$$\begin{aligned}
& - \frac{6614382034523125 \log(5)}{1072963584} - \frac{1044921875 \gamma_E \log(5)}{1008} - \frac{1044921875 \log(2) \log(5)}{1008} \\
& - \frac{1044921875 \log^2(5)}{2016} - \frac{1107664826873969 \log(7)}{109486080} + 30424 \zeta(3) \Big) e^4 + \dots \Big], \tag{4.39}
\end{aligned}$$

$$\begin{aligned}
\Delta\psi_{7L}^y &= \frac{1}{(1-e^2)^7} \left(\frac{1316474014843}{87318000} + \frac{1113254013233e^2}{9702000} + \frac{7684310037263e^4}{46569600} + \frac{1050560559599e^6}{55883520} \right. \\
& - \frac{21719805083e^8}{1411200} - \frac{52587594569e^{10}}{88704000} + \frac{1815476071e^{12}}{5376000} + \frac{501487361e^{14}}{1290240} \\
& \left. + \frac{37402636549e^{16}}{103219200} + \dots \right) + 4 \left[\gamma_E + \log \left(\frac{8(1-e^2)}{1+\sqrt{1-e^2}} \right) \right] \Delta\psi_{7L2}^y + \Delta\psi_{7L}^{y,x}, \tag{4.40}
\end{aligned}$$

$$\begin{aligned}
\Delta\psi_{7L}^{y,x} &= \frac{1}{(1-e^2)^7} \left[\left(\frac{602624 \log(2)}{225} - \frac{468018 \log(3)}{175} \right) + \left(- \frac{155814256 \log(2)}{1575} + \frac{7956306 \log(3)}{175} \right) e^2 \right. \\
& + \left(\frac{865090292 \log(2)}{525} - \frac{262324089 \log(3)}{800} - \frac{1044921875 \log(5)}{2016} \right) e^4 + \left(- \frac{7561620022 \log(2)}{525} \right. \\
& - \frac{418174083 \log(3)}{200} + \frac{11494140625 \log(5)}{1512} \Big) e^6 + \left(\frac{27112112493049 \log(2)}{283500} \right. \\
& + \frac{339134405423319 \log(3)}{7168000} - \frac{238205615234375 \log(5)}{4644864} - \frac{507989081563901 \log(7)}{27648000} \Big) e^8 \\
& + \left(- \frac{2438441188502 \log(2)}{3375} - \frac{2457755729168913 \log(3)}{7168000} + \frac{328215185546875 \log(5)}{1548288} \right. \\
& + \frac{507989081563901 \log(7)}{1843200} \Big) e^{10} + \left(\frac{27531157668664681 \log(2)}{4961250} + \frac{6481474893571248729 \log(3)}{8028160000} \right. \\
& - \frac{2822922907568359375 \log(5)}{4682022912} - \frac{92389498231271366573 \log(7)}{47775744000} \Big) e^{12} \\
& + \left(- \frac{20936989659899360021 \log(2)}{625117500} + \frac{171956257323847250841 \log(3)}{28098560000} \right. \\
& + \frac{510786718173828125 \log(5)}{16387080192} + \frac{1009210224594126146977 \log(7)}{119439360000} \Big) e^{14} \\
& + \left(\frac{4619194353324708185237 \log(2)}{30005640000} - \frac{982128291923792960826417 \log(3)}{14386462720000} \right. \\
& + \frac{2383328610155127138671875 \log(5)}{134242960932864} - \frac{18946304992805061334986887 \log(7)}{733835427840000} \\
& \left. - \frac{1053921396311414387134166987 \log(11)}{251705551749120000} \right) e^{16} + \dots \Big], \tag{4.41}
\end{aligned}$$

$$\Delta\psi_{7L2}^y = \frac{1}{(1-e^2)^7} \left(- \frac{849152}{1575} - \frac{1804876e^2}{525} - \frac{406921e^4}{105} - \frac{543667e^6}{630} - \frac{10593e^8}{560} \right). \tag{4.42}$$

Since the 7PN $\log^2 y$ term is the next appearance of a leading log, its polynomial part is the same as that in (4.19).

Like (4.20), the 7.5PN term is a rational-number infinite series (times a factor of π), but carries an eccentricity singular factor in its y expansion

$$\begin{aligned}
\Delta\psi_{15/2}^y &= \frac{\pi}{(1-e^2)^{15/2}} \left(\frac{2782895449}{2910600} + \frac{5474927197931e^2}{279417600} + \frac{2889497460734527e^4}{30177100800} + \frac{14129642056150403e^6}{131681894400} \right. \\
& + \frac{264436406564274949e^8}{10534551552000} + \frac{4865872318328300473e^{10}}{3973030871040000} + \frac{31810210018353273131e^{12}}{93445686086860800} \\
& \left. + \frac{19417529285629606991939e^{14}}{104659168417284096000} + \frac{30282407545500635935687e^{16}}{261647921043210240000} + \dots \right). \tag{4.43}
\end{aligned}$$

The breakdown of the 8PN term is discussed prior to the presentation of (4.21), (4.22), (4.23), and (4.24). As mentioned there, the 8PN non-log term is too complex to recite in its entirety here, and its complete form is relegated

to the online repositories [50, 51]. We find

$$\begin{aligned}
\Delta\psi_8^y = & \frac{1}{(1-e^2)^8} \left[\left(\frac{78550205239878250993769}{28193459374080000} - \frac{1888832198890393\gamma_E}{15891876000} + \frac{177306208\gamma_E^2}{11025} \right. \right. \\
& + \frac{569460279231731\pi^2}{123312537600} - \frac{623848083842333\pi^4}{21474836480} - \frac{41942063811247\log(2)}{1059458400} + \frac{2720192\gamma_E\log(2)}{11025} \\
& - \frac{520925728\log^2(2)}{11025} - \frac{868469344973829\log(3)}{3139136000} + \frac{59742279\gamma_E\log(3)}{1225} + \frac{59742279\log(2)\log(3)}{1225} \\
& + \frac{59742279\log^2(3)}{2450} + \frac{8570767578125\log(5)}{96864768} + \frac{678223072849\log(7)}{92664000} - \frac{861696\zeta(3)}{35} \Big) \\
& + \left(\frac{237475489990768636607921}{14096729687040000} - \frac{14786129411817037\gamma_E}{7945938000} + \frac{2189268344\gamma_E^2}{11025} - \frac{270260435561795257\pi^2}{739875225600} \right. \\
& - \frac{10607716992396567\pi^4}{85899345920} - \frac{93307044107449223\log(2)}{7945938000} + \frac{7769433776\gamma_E\log(2)}{2205} + \frac{71130150712\log^2(2)}{11025} \\
& + \frac{152737472062641771\log(3)}{20090470400} - \frac{14061034377\gamma_E\log(3)}{19600} - \frac{14061034377\log(2)\log(3)}{19600} - \frac{14061034377\log^2(3)}{39200} \\
& + \frac{129625141640625\log(5)}{803618816} - \frac{3173828125\gamma_E\log(5)}{7056} - \frac{3173828125\log(2)\log(5)}{7056} - \frac{3173828125\log^2(5)}{14112} \\
& - \frac{55100101995388051\log(7)}{23721984000} - \frac{11326048\zeta(3)}{35} \Big) e^2 + \left(\frac{68813273776486435836697}{2349454947840000} \right. \\
& - \frac{277281064009878713\gamma_E}{42378336000} + \frac{1901024351\gamma_E^2}{3675} - \frac{3710687926688801501\pi^2}{2959500902400} - \frac{6040266216599961\pi^4}{85899345920} \\
& - \frac{38415494517661133\log(2)}{4953312000} - \frac{229436469566\gamma_E\log(2)}{4725} - \frac{452086054463\log^2(2)}{4725} \\
& - \frac{13361781707223294483\log(3)}{200904704000} - \frac{84652534863\gamma_E\log(3)}{78400} - \frac{556288707663\log(2)\log(3)}{78400} - \frac{84652534863\log^2(3)}{156800} \\
& - \frac{13614478243421620625\log(5)}{130186248192} + \frac{2022790234375\gamma_E\log(5)}{84672} + \frac{2022790234375\log(2)\log(5)}{84672} \\
& + \frac{2022790234375\log^2(5)}{169344} + \frac{16555297172261766443\log(7)}{142331904000} - \frac{31036266\zeta(3)}{35} \Big) e^4 + \dots \Big], \tag{4.44}
\end{aligned}$$

$$\begin{aligned}
\Delta\psi_{8L}^y = & \frac{1}{(1-e^2)^8} \left(-\frac{1884153630595993}{31783752000} - \frac{14577716249419597e^2}{15891876000} - \frac{263990606631280313e^4}{84756672000} \right. \\
& - \frac{317009475999791347e^6}{101708006400} - \frac{35185381628335093e^8}{50854003200} - \frac{2054145845907949e^{10}}{226017792000} - \frac{6410920059013081e^{12}}{193729536000} \\
& - \frac{18165080552837e^{14}}{677376000} - \frac{10104654253231e^{16}}{481689600} + \dots \Big) + 4 \left[\gamma_E + \log \left(\frac{8(1-e^2)}{1+\sqrt{1-e^2}} \right) \right] \Delta\psi_{8L2}^y + \Delta\psi_{8L}^{y,x} \\
\Delta\psi_{8L}^{y,x} = & \frac{1}{(1-e^2)^8} \left[\left(-\frac{70650464\log(2)}{2205} + \frac{59742279\log(3)}{2450} \right) + \left(\frac{2149292536\log(2)}{1575} - \frac{14061034377\log(3)}{39200} \right. \right. \\
& - \frac{3173828125\log(5)}{14112} \Big) e^2 + \left(-\frac{837246081799\log(2)}{33075} - \frac{84652534863\log(3)}{156800} + \frac{2022790234375\log(5)}{169344} \right) e^4 \\
& + \left(\frac{1794465193714\log(2)}{6615} + \frac{77888690488341\log(3)}{716800} - \frac{2564871143359375\log(5)}{16257024} \right. \\
& - \frac{8816899947037\log(7)}{331776} \Big) e^6 + \left(-\frac{21709548541867099\log(2)}{7938000} - \frac{296896914153644769\log(3)}{200704000} \right. \\
& + \frac{142848309056640625\log(5)}{130056192} + \frac{299112464634116791\log(7)}{331776000} \Big) e^8 + \dots \Big], \tag{4.45}
\end{aligned}$$

$$\Delta\psi_{8L2}^y = \frac{1}{(1-e^2)^8} \left(\frac{44326552}{11025} + \frac{547317086e^2}{11025} + \frac{1901024351e^4}{14700} + \frac{394272401e^6}{4410} + \frac{2037624299e^8}{141120} + \frac{7800417e^{10}}{31360} \right). \tag{4.46}$$

C. Discussion

By extending the calculation of the spin-precession invariant to a high order (e^{16}) in eccentricity, the expansions presented in the previous two subsections, when viewed by PN order, reveal eccentricity dependence that has parallels with that seen in the energy and angular momentum fluxes [2–4] and in the redshift invariant [6]. The first three PN orders are closed in form and were found previously [18]. It is at 4PN to 9PN that our work makes new contributions. At 4PN order the first appearance of a logarithmic term [18] occurs. Not surprisingly given past experience and the fact that the 4PN log term is a leading log [2], we find it also has a closed-form expression.

The 4PN log function then reappears in the 4PN non-log part when we regroup, or resum, that term. This is not merely a trivial exercise, since the occurrence of the 4PN log term in the non-log part gathers together all of the dependence that is logarithmic in the eccentricity as well as the appearance of the Euler-Mascheroni constant γ_E . This regrouping is directly analogous to what proved possible in the redshift invariant [6] and the fluxes [1, 3]. Next, once terms are grouped on π^2 , we see another closed-form function of e emerge.

The remaining transcendental numbers in $\Delta\psi_4$, which we group into a term called $\Delta\psi_4^X$, have a form that resembles the 3PN energy flux function $\chi(e)$ [2, 52]. The coefficients in $\chi(e)$ can be calculated to arbitrary order [15]. We showed previously [6] a special function ($\Lambda_0(e)$) that provides complete knowledge of the analogous χ -like function in the 4PN redshift invariant. It is possible that PN theory analysis might reveal a similar special function for $\Delta\psi_4^X$ that is based on the Newtonian quadrupole moment power spectrum [2], but we have yet to find it. Note that in the y -based PN expansion, an eccentricity function that appears to make the series converge as $e \rightarrow 1$ can be isolated from $\Delta\psi_{4L}^X$ by pulling out the function $-3\log(1 - e^2)\Delta\psi_{4L}$. This procedure was first learned in working with the fluxes and redshift (see [2, 15] for more information). What remains in the 4PN non-log term is (apparently) an infinite series with rational coefficients. It is surprising that this part could not (yet) be manipulated into a closed form, as was possible in the fluxes and redshift invariant.

At 5PN and 6PN we again found closed-form expressions in the log parts. Once the log terms are known, they assist in allowing the 5PN and 6PN non-log parts to be segregated into important functional groupings like that found at 4PN, though with increasing complexity.

7PN order marks the first appearance of a $\log^2 y$, making it the next term in the (integer-order) leading-log sequence. This $\Delta\psi_{7L2}$ term is also found to be closed in form. The connection between $\Delta\psi_{7L2}$ and $\Delta\psi_{7L}$ then is seen to closely mirror the connection between $\Delta\psi_{4L}$ and $\Delta\psi_4$. This is exactly analogous to what occurs in the redshift invariant at 7PN order (see [6] for the connection in the redshift invariant and [2] for a detailed description of

leading-logarithmic terms in the fluxes).

Finally, we note that half-integer contributions begin at 5.5PN order, an infinite series with rational-number coefficients. This contribution marks the first term in the half-integer leading-log sequence. The next two half-integer PN terms (6.5PN and 7.5PN) are likewise series with rational coefficients. The next half-integer contribution after that, at 8.5PN order (found in the repositories [50, 51]), contains a log term, which is expected of the second element in the half-integer leading-log sequence.

D. Comparison to numerical data on close orbits

The usefulness of these high-order PN expansions in reaching into the high-speed, strong-field regime can be assessed by comparing their numerical evaluation to the numerical spin-precession invariant data given in the extensive table (Table II) of [18]. We compare both our $1/p$ and y PN expansions, along with a few additional basic resummations applied to each. For example, see [1, 53, 54] on creating one PN series from another, like reciprocal and exponential resummation. Our results for a pair of orbital sizes, $p = 10$ and $p = 20$, and a pair of eccentricities, $e = 0.1$ and $e = 0.25$, are provided in Fig. 1.

All of the series exhibit fairly strong convergence for the case $p = 20$, reaching a fractional error better than 10^{-5} for both $e = 0.1$ and $e = 0.25$ using 9PN terms. The dataset in [18] is restricted to $e \leq 0.25$, limiting our ability to test the expansions at higher eccentricities. The experience with numerical comparisons of the redshift invariant [6] suggests that our series will remain viable up to $e \simeq 0.5$ at $p = 20$. At the closer separation of $p = 10$ the convergence is markedly slower, attaining relative errors near 1% at both $e = 0.1$ and $e = 0.25$. This observation is consistent with the analysis in [20], who showed that the series is expected to diverge at a larger radius than the redshift invariant (i.e., at the separatrix, as opposed to the light ring). Moreover, the basic resummation methods we have tried have not substantially improved the convergence.

Fig. 2 shows how the fractional errors behave versus eccentricity e when using a set of series that have been truncated at different PN orders. We see that knowledge gained from our calculation of the spin-precession invariant through e^{16} provides series that converge uniformly over a range of eccentricity through $e = 0.25$. The curves strongly suggest that our PN series will remain accurate as $e \rightarrow 0.5$ or more. The current version of our code could reach higher PN order but at the expense of reducing the order of the expansion in e , for example perhaps reaching 12PN and e^{10} . In any event, if we consider the task of modeling EMRIs, conservative dynamical effects are suppressed by a factor of the mass ratio relative to the secular effect of the gravitational wave fluxes [28]. Thus, our present depth of PN expansion of the spin-precession invariant is likely adequate for giving its contribution to

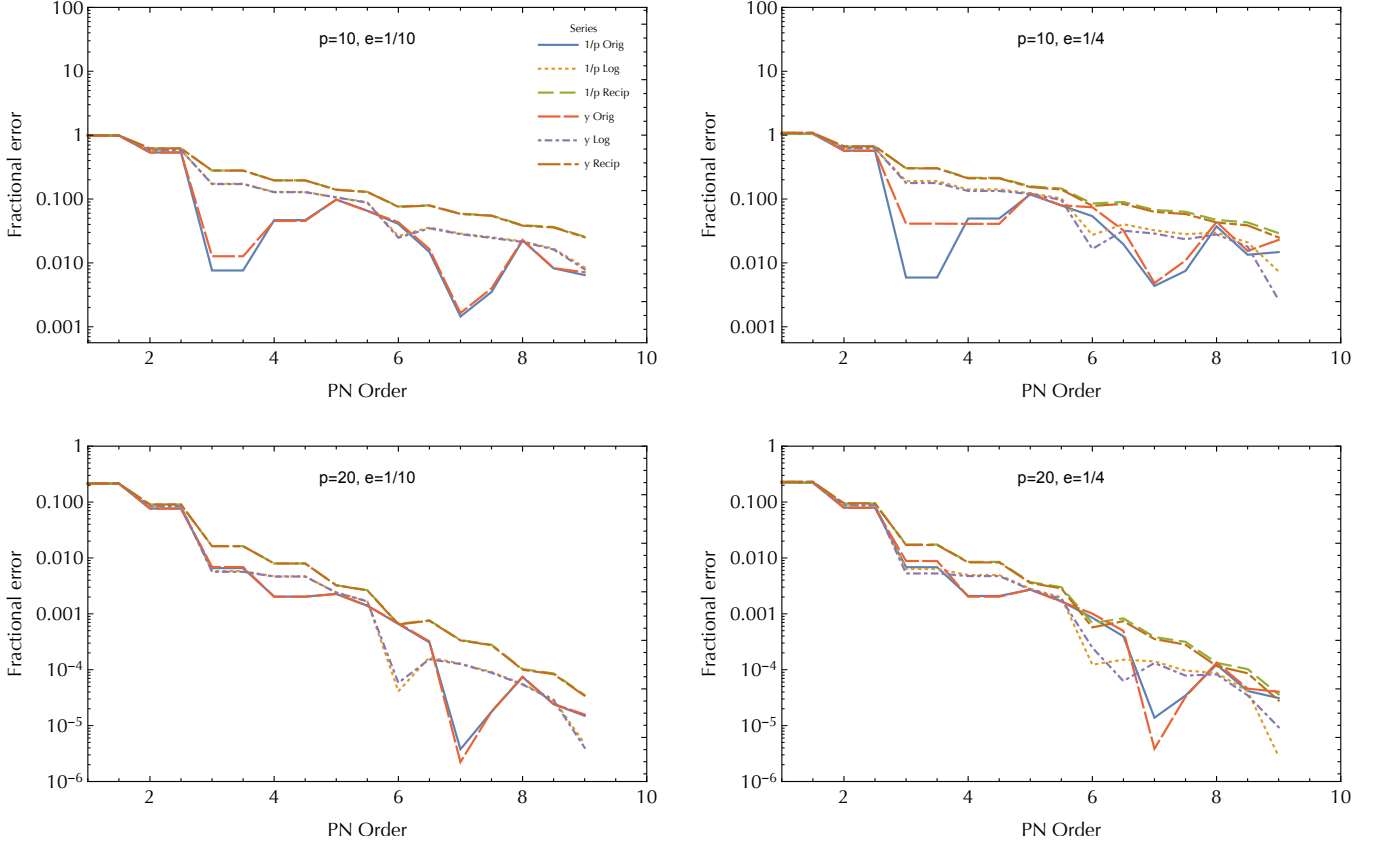


FIG. 1. Accuracy of the spin-precession invariant PN expansion and its resummations for several individual orbits. The numerical values of our redshift expansion are plotted against data from [18] for the orbits $(p = 10, e = 1/10)$, $(p = 10, e = 1/4)$, $(p = 20, e = 1/10)$, $(p = 20, e = 1/4)$. Within each plot comparisons are made for both the $1/p$ and y expansions, both with and without the use of logarithmic and reciprocal summations. Note the changes in vertical scaling in the bottom two plots.

EMRI dynamics.

V. CONCLUSIONS

We have presented the PN and eccentricity expansion of the spin-precession invariant ψ at first order in the mass ratio for a point mass in bound eccentric motion about a Schwarzschild black hole. The RWZ formalism is used, calculating the metric perturbation and self-force in Regge-Wheeler gauge. The calculation is completely analytic, using a MATHEMATICA code and drawing upon the analytic PN expansion of the MST formalism and the general- l expansion ansatz of [10, 14]. The construction and regularization of the spin-precession invariant follows methods used by [18–20], as well as simplifications of the eccentricity dependence developed in our previous work [1, 6]. We have computed the spin-precession invariant to 9PN (which has been done before [20, 21]) but have calculated the eccentricity expansion to e^{16} (with one exception, 4PN, which is calculated to e^{30}), far beyond the order e^2 results previously known.

The high-order eccentricity expansions led to the discovery of five new closed-form expressions, for $\Delta\psi_{4L}$, $\Delta\psi_{5L}$, $\Delta\psi_{6L}$, $\Delta\psi_{7L2}$, and $\Delta\psi_{8L2}$. In addition, we were able to use the methods developed in our past work on the gravitational wave fluxes [2–4] and the redshift invariant [6] to segregate the eccentricity dependence of many of the other PN terms into significant functional parts and to identify eccentricity singular factors that aid convergence in the $e \rightarrow 1$ limit. The PN series results were compared to prior numerical calculations, and shown to exhibit fractional errors in convergence of around 10^{-5} for orbital separation of $p = 20$ and of around 10^{-2} for $p = 10$.

The expansions of $\Delta\psi$ could be extended further. The bottleneck step in the calculation is the expansion of the general- l , even-parity normalization constant C_{lmn}^+ , which requires about 7 days on the UNC Longleaf cluster to reach 10PN (relative) order and e^{20} . Beyond simply committing more resources or finding a faster cluster, intermediate expansions, which sacrifice PN order for higher order in eccentricity or vice versa, can be obtained immediately and may be useful. As we described, by fo-

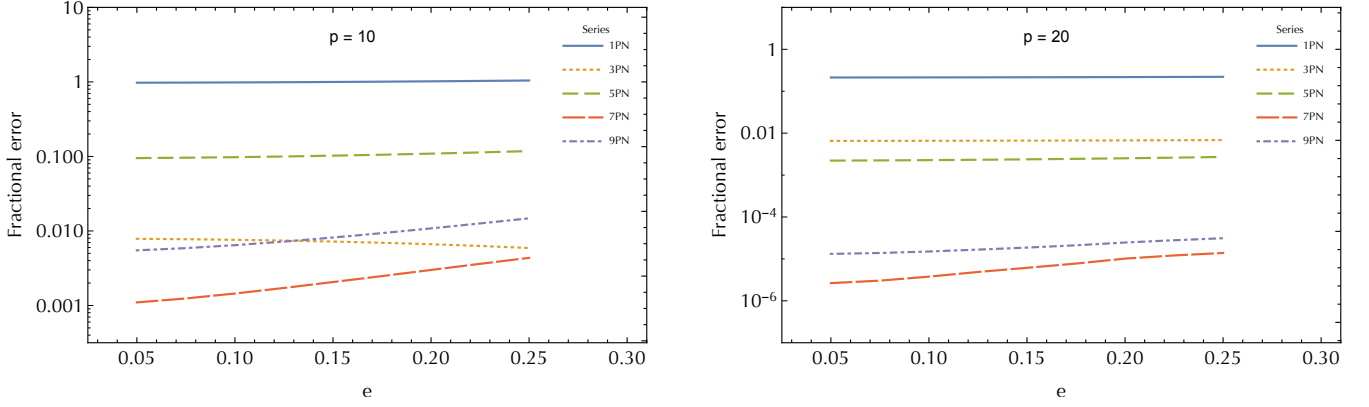


FIG. 2. Accuracy of the spin invariant PN expansion with increasing e . The (simple) $1/p$ expansion is compared to numerical data for the e values 0.05 to 25 at 0.05 intervals (plots are made continuous for clarity) for both $p = 10$ and $p = 20$.

cusing on one PN order (4PN), we were able to push the eccentricity expansion to e^{30} .

It will be useful now to translate these expansions to their equivalent quantities within the EOB formalism. EOB waveforms have been crucial to the success of LIGO data analysis and will likely contribute to deciphering LISA detections. The spin-precession invariant in first-order self-force calculations can be transcribed to yield portions of the EOB gyrogravitomagnetic ratio $g_{S*}(1/r; p_r; p_\varphi)$, by extending a procedure described in [19]. However, the process is lengthy, with each new order in e^2 requiring cumbersome derivations, and we leave that process for future work.

ACKNOWLEDGMENTS

We thank Chris Kavanagh for helpful discussions concerning intermediate steps in the expansion procedure. This work was supported by NSF Grant Nos. PHY-1806447 and PHY-2110335 to the University of North Carolina–Chapel Hill. C.M.M. acknowledges additional support from NASA ATP Grant 80NSSC18K1091 to MIT.

-
- [1] C. Munna, Phys. Rev. D **102**, 124001 (2020), arXiv:2008.10622 [gr-qc].
 - [2] C. Munna and C. R. Evans, Phys. Rev. D **100**, 104060 (2019), arXiv:1909.05877 [gr-qc].
 - [3] C. Munna, C. R. Evans, S. Hopper, and E. Forseth, Phys. Rev. D **102**, 024047 (2020), arXiv:2005.03044 [gr-qc].
 - [4] C. Munna and C. R. Evans, Phys. Rev. D **102**, 104006 (2020), arXiv:2009.01254 [gr-qc].
 - [5] C. Munna and C. R. Evans, to be submitted to Phys. Rev. D (2022).
 - [6] C. Munna and C. R. Evans, arXiv e-prints, arXiv:2203.13832 (2022), arXiv:2203.13832 [gr-qc].
 - [7] T. Regge and J. Wheeler, Phys. Rev. **108**, 1063 (1957).
 - [8] F. Zerilli, Phys. Rev. D **2**, 2141 (1970).
 - [9] S. Mano, H. Suzuki, and E. Takasugi, Progress of Theoretical Physics **96**, 549 (1996), gr-qc/9605057.
 - [10] D. Bini and T. Damour, Phys. Rev. D **87**, 121501 (2013), arXiv:1305.4884 [gr-qc].
 - [11] D. Bini and T. Damour, Phys. Rev. D **89**, 064063 (2014), arXiv:1312.2503 [gr-qc].
 - [12] D. Bini and T. Damour, Phys. Rev. D **90**, 024039 (2014), arXiv:1404.2747 [gr-qc].
 - [13] D. Bini and T. Damour, Phys. Rev. D **90**, 124037 (2014), arXiv:1409.6933 [gr-qc].
 - [14] C. Kavanagh, A. C. Ottewill, and B. Wardell, Phys. Rev. D **92**, 084025 (2015), arXiv:1503.02334 [gr-qc].
 - [15] E. Forseth, C. R. Evans, and S. Hopper, Phys. Rev. D **93**, 064058 (2016).
 - [16] S. Hopper, C. Kavanagh, and A. C. Ottewill, Phys. Rev. D **93**, 044010 (2016), arXiv:1512.01556 [gr-qc].
 - [17] S. R. Dolan, N. Warburton, A. I. Harte, A. Le Tiec, B. Wardell, and L. Barack, Phys. Rev. D **89**, 064011 (2014), arXiv:1312.0775 [gr-qc].
 - [18] S. Akcay, D. Dempsey, and S. Dolan, Class. Quant. Grav. **34**, 084001 (2017), arXiv:1608.04811v3 [gr-qc].
 - [19] C. Kavanagh, D. Bini, T. Damour, S. Hopper, A. Ottewill, and B. Wardell, Phys. Rev. D **96**, 064012 (2017), 10.1103/PhysRevD.96.064012, arXiv:1706.00459 [gr-qc].
 - [20] D. Bini, T. Damour, and A. Gericco, Phys. Rev. D **97**, 104046 (2018), arXiv:1801.03704 [gr-qc].
 - [21] D. Bini and A. Gericco, Phys. Rev. D **100**, 104003 (2019), arXiv:1907.11082 [gr-qc].
 - [22] L. Barack, T. Damour, and N. Sago, Phys. Rev. D **82**, 084036 (2010), arXiv:1008.0935 [gr-qc].
 - [23] A. Le Tiec, L. Blanchet, and B. Whiting, Phys. Rev. D **85**, 064039 (2012), arXiv:1111.5378.
 - [24] D. Bini, T. Damour, and A. Gericco, Phys. Rev. D **93**, 064023 (2016), arXiv:1511.04533 [gr-qc].

- [25] D. Bini, T. Damour, and A. Geralico, Phys. Rev. Lett. **123**, 231104 (2019), arXiv:1909.02375 [gr-qc].
- [26] D. Bini, T. Damour, and A. Geralico, (2020), arXiv:2003.11891 [gr-qc].
- [27] D. Bini, T. Damour, and A. Geralico, (2020), arXiv:2004.05407 [gr-qc].
- [28] T. Hinderer and E. E. Flanagan, Phys. Rev. D **78**, 064028 (2008), arXiv:0805.3337 [gr-qc].
- [29] K. Martel and E. Poisson, Phys. Rev. D **71**, 104003 (2005), arXiv:gr-qc/0502028.
- [30] M. Sasaki and H. Tagoshi, Living Reviews in Relativity **6**, 6 (2003), gr-qc/0306120.
- [31] C. Darwin, Proc. R. Soc. Lond. A **249**, 180 (1959).
- [32] C. Cutler, D. Kennefick, and E. Poisson, Phys. Rev. D **50**, 3816 (1994).
- [33] L. Barack and N. Sago, Phys. Rev. D **81**, 084021 (2010), arXiv:1002.2386 [gr-qc].
- [34] S. Hopper, E. Forseth, T. Osburn, and C. R. Evans, Phys. Rev. D **92**, 044048 (2015), arXiv:1506.04742 [gr-qc].
- [35] I. S. Gradshteyn, I. M. Ryzhik, A. Jeffrey, and D. Zwillinger, *Table of Integrals, Series, and Products, Seventh Edition Elsevier Academic Press, 2007. ISBN 012-373637-4* (2007).
- [36] S. Hopper and C. R. Evans, Phys. Rev. D **82**, 084010 (2010).
- [37] S. Chandrasekhar, Royal Society of London Proceedings Series A **343**, 289 (1975).
- [38] S. Chandrasekhar and S. Detweiler, Royal Society of London Proceedings Series A **345**, 145 (1975).
- [39] S. Chandrasekhar, *The Mathematical Theory of Black Holes*, The International Series of Monographs on Physics, Vol. 69 (Clarendon, Oxford, 1983).
- [40] M. Berndston, *Harmonic Gauge Perturbations of the Schwarzschild Metric*, Ph.D. thesis, University of Colorado (2007), arXiv:0904.0033v1.
- [41] L. Barack, A. Ori, and N. Sago, Phys. Rev. D **78**, 084021 (2008), arXiv:0808.2315.
- [42] N. Sago, L. Barack, and S. L. Detweiler, Phys. Rev. D **78**, 124024 (2008), arXiv:0810.2530 [gr-qc].
- [43] J. A. Marck, Proceedings of the Royal Society of London Series A **385**, 431 (1983).
- [44] R. M. Cheng and C. R. Evans, Phys. Rev. D **87**, 104010 (2013), arXiv:1303.4129 [gr-qc].
- [45] L. Barack and N. Sago, Phys. Rev. D **83**, 084023 (2011), arXiv:1101.3331 [gr-qc].
- [46] B. Wardell and N. Warburton, Phys. Rev. D **92**, 084019 (2015), arXiv:1505.07841 [gr-qc].
- [47] S. L. Detweiler and B. F. Whiting, Phys. Rev. D **67**, 024025 (2003), arXiv:gr-qc/0202086.
- [48] L. Barack and A. Ori, Phys. Rev. D **64**, 124003 (2001), arXiv:gr-qc/0107056.
- [49] J. Thompson, B. Wardell, and B. Whiting, Phys. Rev. D **99**, 124046 (2019), 10.1103/PhysRevD.99.124046, arXiv:1811.04432 [gr-qc].
- [50] “Black Hole Perturbation Toolkit,” bhptoolkit.org.
- [51] “UNC Gravitational Physics Group,” <https://github.com/UNC-Gravitational-Physics>.
- [52] K. G. Arun, L. Blanchet, B. R. Iyer, and M. S. S. Quisailah, Phys. Rev. D **77**, 064034 (2008), arXiv:0711.0250 [gr-qc].
- [53] S. Isoyama, R. Fujita, H. Nakano, N. Sago, and T. Tanaka, Progress of Theoretical and Experimental Physics **2013**, 063E01 (2013), arXiv:1302.4035 [gr-qc].
- [54] N. K. Johnson-McDaniel, Phys. Rev. D **90**, 024043 (2014), arXiv:1405.1572 [gr-qc].